



Study of final-state radiation in decays of Z bosons produced in pp collisions at 7 TeV

The CMS Collaboration*

Abstract

The differential cross sections for the production of photons in $Z \rightarrow \mu^+ \mu^- \gamma$ decays are presented as a function of the transverse energy of the photon and its separation from the nearest muon. The data for these measurements were collected with the CMS detector and correspond to an integrated luminosity of 4.7 fb^{-1} of pp collisions at $\sqrt{s} = 7 \text{ TeV}$ delivered by the CERN LHC. The cross sections are compared to simulations with POWHEG and PYTHIA, where PYTHIA is used to simulate parton showers and final-state photons. These simulations match the data to better than 5%.

Published in Physical Review D as doi:10.1103/PhysRevD.91.092012.

1 Introduction

We present a study and differential cross section measurements of photons emitted in decays of Z bosons produced at a hadron collider. Such radiative decays of the Z boson were noted in the very first Z boson publications of UA1 and UA2 [1, 2], but subsequently have not been given a detailed study in hadron colliders. In 2011, the CERN LHC delivered pp collisions at $\sqrt{s} = 7\text{ TeV}$, and data corresponding to an integrated luminosity of 4.7 fb^{-1} were collected with the CMS detector. From these data, we select a sample of events in which a Z boson decays to a $\mu^+\mu^-$ pair and an energetic photon. We measure the differential cross sections $d\sigma/dE_T$ with respect to the photon transverse energy E_T and $d\sigma/d\Delta R_{\mu\gamma}$ with respect to the separation of the photon from the nearest muon. Here, $\Delta R_{\mu\gamma} = \sqrt{(\phi_\mu - \phi_\gamma)^2 + (\eta_\mu - \eta_\gamma)^2}$, where ϕ is the azimuthal angle (in radians) around the beam axis and η is the pseudorapidity. The cross sections include contributions from the Z resonance, virtual photon exchange, and their interference, collectively referred to as Drell–Yan (DY) production.

Photons emitted in Z boson decays, which we call final state radiation (FSR) photons, can be energetic (tens of GeV) and well separated from the leptons (by more than a radian). Quantum electrodynamics (QED) corrections that describe FSR production are well understood. Quantum chromodynamics (QCD) corrections modify the kinematic distributions of the Z boson; in particular, the Z boson acquires a nonzero component of momentum transverse to the beam: $q_T > 0$. The FEWZ program calculates both QCD and QED corrections for the DY process [3]. However, it does not include mixed QCD and QED corrections; the required two-loop integrals are technically very challenging, and progress has been made only recently [4]. In practice, event generators employing matrix element calculations matched to parton showers must be used [5, 6]. It is the goal of this analysis to establish the quality of the modeling of FSR over a wide kinematic and angular range. The results will support future measurements of the W mass, the study of Z + γ production, and searches for new particles in final states with photons.

In an attempt to compare photons emitted close to a muon (a process that is modeled primarily by a partonic photon shower) and far from the muons (which requires a matrix element calculation), we measure $d\sigma/dE_T$ for $0.05 < \Delta R_{\mu\gamma} \leq 0.5$ and $0.5 < \Delta R_{\mu\gamma} \leq 3$. Furthermore, since the size of the QCD corrections varies with the transverse momentum of the Z boson, we measure $d\sigma/dE_T$ and $d\sigma/d\Delta R_{\mu\gamma}$ for $q_T < 10\text{ GeV}$ and $q_T > 50\text{ GeV}$, where q_T is defined as the vector sum of the transverse momenta of the two muons and the photon. These cross sections are defined with respect to the fiducial and kinematic requirements detailed below; no acceptance corrections are applied. Nonetheless, we do correct for detector resolution and efficiencies.

This article is structured as follows. We briefly describe the CMS detector and the event samples we use in Section 2. The details of the event selection are given in Section 3. Background estimation and the way we unfold the data distributions are discussed in Sections 4 and 5. We discuss the systematic uncertainties in Section 6 and report our results and summarize the work in Sections 7 and 8.

2 The CMS detector and event samples

A full description of the CMS detector can be found in Ref. [7]; here we briefly describe the components most important for this analysis. The central feature of the CMS experiment is a superconducting solenoid that provides an axial magnetic field of 3.8 T. A tracking system

composed of a silicon pixel detector and a silicon strip detector is installed around the beam line, and provides measurements of the trajectory of charged particles for $|\eta| < 2.5$. After passing through the tracker, particles strike the crystal electromagnetic calorimeter (ECAL) followed by the brass and scintillator hadron calorimeter. The solenoid coil encloses the tracker and the calorimetry. Four stations of muon detectors measure the trajectories of muons that pass through the tracker and the calorimeters for $|\eta| < 2.4$. Three detector technologies are employed in the muon system: drift tubes for central rapidities, cathode strip detectors for the forward rapidities, and resistive-plate chambers for all rapidities. Combining information from the muon detectors and the tracker, the transverse momentum (p_T) resolution for muons used in this analysis varies from 1 to 6%, depending on η and p_T [8]. The E_T of photons and electrons is measured using energy deposited in the ECAL, which consists of nearly 76 000 lead tungstate crystals distributed in the barrel region ($|\eta| < 1.479$) and two endcap regions ($1.479 < |\eta| < 3.0$). The photon energy resolution is better than 5% for the range of E_T pertinent to this analysis [9]. Events are selected using a two-level trigger system. The level-1 trigger, composed of custom-designed processing hardware, selects events of interest based on information from the muon detectors and calorimeters [10]. The high-level trigger is software-based, running a simpler and therefore faster version of the offline reconstruction code on the full detector information, including the tracker [11].

Simulated data samples are used to design and verify the principles of the analysis. They are also used to assess efficiencies, resolution, and backgrounds. The signal process is simulated using the POWHEG (V1.0) [12] event generator with PYTHIA (V6.4.24) [13] used to simulate parton showers and final state photons (referred to in what follows as POWHEG+PYTHIA). This combination is also used for $t\bar{t}$ and diboson (WW , WZ , ZZ) production. The CT10 [14] parton distribution functions are used. The Z2 parameter set [15] is used to model the underlying event in PYTHIA, and the effects of additional pp collisions that produce signals registered together with the main interaction are included in the simulation.

The response of the detector is simulated using GEANT4 [16]. The simulated events are processed using the same version of the offline reconstruction code used for the data.

3 Event selection

The data are recorded using a trigger that requires two muons. One muon is required to have $p_T > 13$ GeV, and the other, $p_T > 8$ GeV. This trigger has no requirement on the isolation of the muons.

Events with a pair of oppositely charged, well-reconstructed, and isolated muons and an isolated photon are selected. The kinematic and fiducial requirements for selecting events are based wholly on the muon and photon kinematic quantities, and are summarized in Table 1. As explained below, we use the dimuon mass $M_{\mu\mu}$ to define a “signal region” that is rich in FSR photons, and a “control region” that is dominated by background sources of photons.

Muons are selected in the manner developed for the measurements of the DY cross section [17]. They must be reconstructed using an algorithm that finds a track segment in the muon detectors and links it with a track in the silicon tracker, and also through an algorithm that extrapolates a track in the silicon tracker outward and matches it with hits registered in the muon detectors. We select the two highest p_T muons (which we will call “leading” and “trailing”), and ignore any additional muons. These two muons must have opposite charge. The leading muon must satisfy the requirements $p_T > 31$ GeV and $|\eta| < 2.4$, while the trailing muon must satisfy $p_T > 9$ GeV and $|\eta| < 2.4$ to ensure good reconstruction efficiency. A vertex fit is per-

formed to the two muon tracks, and the χ^2 probability of the fit must be at least 0.02. We define the difference between π and the opening angle of the two muons as the acollinearity α , and remove a very small region of phase space where α is less than 5 mrad to reduce contamination by cosmic rays to a negligible level.

Photons are reconstructed using the particle flow (PF) algorithm [18, 19] that uses clustered energy deposits in ECAL. The PF algorithm allows us to reconstruct photons at relatively low E_T and to maintain coherence with the calculation of the isolation observables described below. Photons that convert to electron-positron pairs are included in this reconstruction. Events selected for this analysis must have at least one photon with $E_T > 5$ GeV, and the separation of this photon with respect to the closest muon must satisfy $0.05 < \Delta R_{\mu\gamma} \leq 3$. Studies using the simulation show that photons with $\Delta R_{\mu\gamma} < 0.05$ are difficult to reconstruct reliably due to the energy deposition left by the muon, and no signal photons with $\Delta R_{\mu\gamma} > 3$ are expected. If an event has more than one photon satisfying this selection criteria, we select the one with the highest E_T . In events in which one photon is selected, a second photon is present 15% of the time; however, these extra photons are expected to be mostly background, since the fraction of events with a second FSR photon in simulation is approximately 0.5%. More details about these background photons are given in Section 4.

Table 1: Summary of kinematic and fiducial event requirements

Object	Requirement
Leading muon	$p_T > 31$ GeV and $ \eta < 2.4$
Trailing muon	$p_T > 9$ GeV and $ \eta < 2.4$
Acollinearity	$\alpha > 0.005$ radians
Photon	$E_T > 5$ GeV, $ \eta < 2.4$ but not $1.4 < \eta < 1.6$; $0.05 < \Delta R_{\mu\gamma} \leq 3$
Signal region	$30 < M_{\mu\mu} < 87$ GeV
Control region	$89 < M_{\mu\mu} < 100$ GeV

All three particles emitted in the Z boson decay—the two muons and the photon—are usually isolated from other particles produced in the same bunch crossing. We can reduce backgrounds substantially by imposing appropriate isolation requirements. The isolation quantities, I_μ for the muons and I_γ for the photon, are based on the scalar p_T sums of reconstructed PF particles within a cone around the muon or photon direction. The cone size for both muons and photons is $\Delta R = 0.3$. The muon p_T is not included in the sum for I_μ , and the photon E_T is not included in the sum for I_γ ; these isolation quantities are meant to represent the energy carried by particles originating from the main primary vertex close to the given muon or photon. For a well-isolated muon or photon, I_μ or I_γ should be small.

Special care is taken to avoid inefficiencies and biases occurring when the FSR photon falls close to the muon; in such cases the muon and the photon may appear, superficially, to be nonisolated. To avoid this effect, we exclude any PF photon from the muon isolation sum. Furthermore, since the photon can convert and produce charged particle tracks that cannot always be unambiguously identified as an e^+e^- pair, we exclude from the muon isolation sum charged tracks that lack hits in the pixel detector or that have $p_T < 0.5$ GeV. Finally, any particle that lands in a cone of $\Delta R < 0.2$ around a PF photon is excluded from the muon isolation sum. After these modifications to the muon isolation variable, the efficiency of the isolation requirement is flat (98%) for all $\Delta R_{\mu\gamma}$ and is higher than the efficiency of the unmodified isolation requirement by about 0.5%. Adding these modifications does not significantly increase the backgrounds.

The instantaneous luminosity of the LHC was sufficiently high that each bunch crossing resulted in multiple pp collisions (8.2 on average). The extraneous pp collisions are referred to as “pileup” and must be taken into consideration when defining and calculating the muon and photon isolation variables. Charged hadrons, electrons, and muons coming from pileup can be identified by checking their point of origin along the beam line, which will typically not coincide with the primary vertex from which the muons originate. When summing the contributions of charged hadrons, electrons, and muons to the isolation variable, those coming from pileup are excluded. This distinction is not possible for photons and neutral hadrons, however. Instead, an estimate I_p of the contribution of photons and neutral hadrons to the sum is made: we use one-half of the (already excluded) contribution from charged hadrons within the isolation cone. This estimate is subtracted from the sum of contributions from photons and neutral hadrons; if the result is negative, we then use a net contribution of zero.

We designate by I_{h^\pm} the sum of p_T for charged particles that are not excluded from the isolation sum. We let I_{em} and I_{h^0} stand for the sums over the p_T of all photons and neutral hadrons, and I_p for the estimate of the pileup contribution to I_{em} and I_{h^0} . The muon isolation variable is, then,

$$I_\mu = (I_{h^\pm} + I_{h^0}) / p_T. \quad (1)$$

Note that the sum is normalized to the p_T of the muon. We require $I_\mu < 0.2$ for both muons.

The photon isolation variable is calculated as above, except that the muons are not included in the sum, and there is no special exclusion of charged tracks near the photon:

$$I_\gamma = I_{h^\pm} + \max(I_{em} + I_{h^0} - I_p, 0). \quad (2)$$

We require $I_\gamma < 6 \text{ GeV}$.

The emission of FSR photons in Z boson decays reduces the momenta of the muons. Consequently, the dimuon mass $M_{\mu\mu}$ tends to be lower than M_Z , the nominal mass of the Z boson. Simulations indicate that, for most of the signal, $M_{\mu\mu} < 87 \text{ GeV}$, due to the requirement $E_T > 5 \text{ GeV}$ for the photon. They also show that the $M_{\mu\mu}$ distribution for radiative decays $Z \rightarrow \mu^+\mu^-\gamma$ ends at $M_{\mu\mu} \approx 30 \text{ GeV}$. A requirement $M_{\mu\mu} > 30 \text{ GeV}$ also helps to avoid a kinematic region in which the acceptance is difficult to model. Therefore, our signal region is defined by $30 < M_{\mu\mu} < 87 \text{ GeV}$. We also define a control region by $89 < M_{\mu\mu} < 100 \text{ GeV}$, where the contribution of FSR photons is quite small (below 0.5%). The numbers of events we select are 56 005 in the signal region and 45 277 in the control region.

4 Background estimation

Nearly all selected events have two prompt muons from the DY process. Backgrounds come mainly from “nonprompt” photons, which may be genuine photons produced in the decays of light mesons (such as π^0 and η), a pair of overlapping photons that cannot be distinguished from a single photon, and photons from pileup. We study these backgrounds with simulated DY events and apply corrections so that the simulation reproduces the data distributions, as described in detail below.

Some events come from processes other than DY, such as $t\bar{t}$ and diboson production. These backgrounds are very small and are estimated using the simulation. Similarly, a small background from the DY production of $\tau^+\tau^-$ is also estimated from simulation. The background from multijet events, including events with a $W^\pm \rightarrow \mu^\pm\nu$ decay, is estimated using events with same-sign muons. Backgrounds from simultaneous nonprompt muon and nonprompt photon sources are negligible. The composition of the signal sample is given in Table 2.

Table 2: Composition of the signal sample. The simulation has been tuned to reproduce the data in the control region.

Process	Fraction
Signal	77.1%
DY with a nonprompt photon	9.5%
Pileup	11.2%
$t\bar{t}$	0.6%
$\tau^+\tau^-$	0.3%
Dibosons	0.2%
Multijets	1.1%

The control region is dominated by nonprompt photons whose kinematic distributions (E_T , η , $\Delta R_{\mu\gamma}$) are nearly identical to nonprompt photons in the signal region. Quantitative comparisons of data and simulation revealed significant discrepancies in the control region that prompted corrections to the simulation, which we now explain.

The POWHEG+PYTHIA sample does not reproduce the number of jets per event well, so we apply weights to the simulated events as a function of the number of reconstructed jets in each event. For this purpose, jets are reconstructed from PF objects using the anti- k_T algorithm [20] with a size parameter $R = 0.5$. We consider jets with $p_T > 20$ GeV and $|\eta| < 2.4$ that do not overlap with the muons or the photon.

Studies of I_γ for events in the control region reveal small discrepancies in the multiplicity and p_T spectra of charged hadrons included in the sum. We apply weights to the simulated events to bring the multiplicities into agreement, and we impose $p_T > 0.5$ GeV on charged hadrons. The simulated I_γ distributions match those in data very well after applying these weights.

Finally, the E_T and η distributions of nonprompt photons in the simulation deviate from those in the data. We fit simple analytic functions to the ratios of data to simulated E_T and η distributions and define a weight as the product of those functions. We check that this factorization is valid (i.e., that the E_T correction is the same for different narrow ranges of η , and vice versa).

After these three corrections (for jet multiplicity, for the spectrum of charged hadrons in the isolation sums, and for the E_T and η of the nonprompt photon), the simulation matches the data in all kinematic distributions in the control region, an example of which is shown in Fig. 1, left. The total change in the background estimate due to these corrections is approximately 5 to 10%. We use the simulation with these weights to model the small background in the signal region (Fig. 1, right).

Given the definition of the signal region, the contribution of photons emitted in the initial state is very small (on the order of 4×10^{-4} as determined from the POWHEG+PYTHIA sample) and is counted as signal.

5 Correcting for detector effects

Our goal is to measure differential cross sections in a form that is optimal for testing FSR calculations. Therefore we are obliged to remove the effects of detector resolution and efficiency (including reconstruction, isolation, and trigger efficiency). The corrections for the muons follow the techniques developed for the DY cross section measurements [17]. The corrections for photons are applied using an unfolding technique, as discussed in this section.

We apply small corrections to the muon momentum scale as a function of muon p_T , η_μ , and

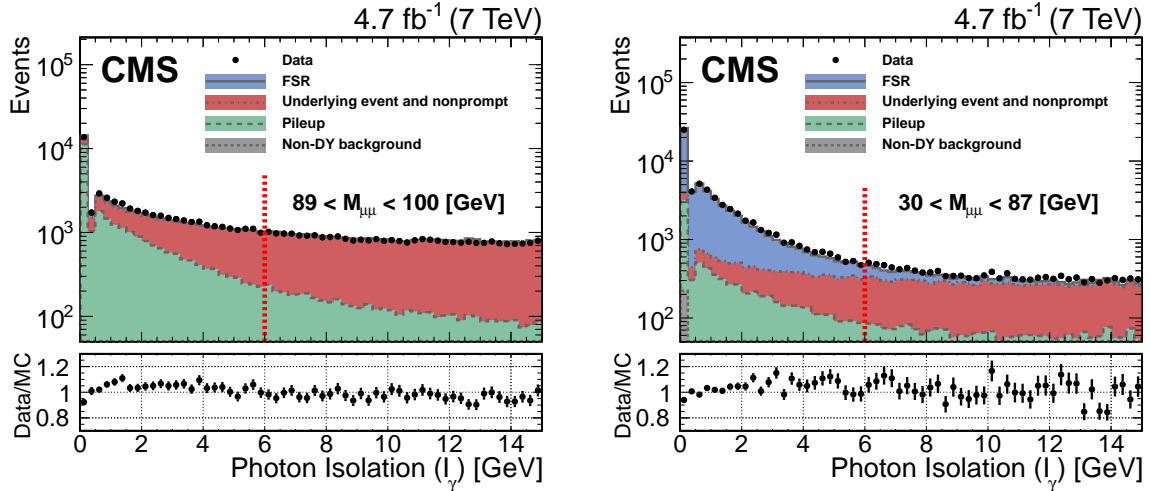


Figure 1: Distributions of the photon isolation variable I_γ for the control region (left) and for the signal region (right) after all corrections have been applied. The bottom panels display the ratio of data to the MC expectation. The requirement for FSR photons is $I_\gamma < 6$ GeV.

ϕ_μ [21]; they have almost no impact on our measurements. The muon reconstruction efficiency, (taken from simulation and corrected to match the data as a function of p_T and η_μ) is taken into account by applying weights on a per-event basis. We do not correct for the approximately 0.5% increase in the isolation efficiency coming from the way we handle FSR photons falling within the muon isolation cone.

The energy scale and efficiencies for photons are more central to our task. Most PF photon energies correspond to the true energies within a few percent. However, in about 13% of the cases the photon energy is significantly underestimated. The simulation reproduces this effect very well. We construct a “response” matrix that relates the PF energy to the true energy as a function of η_γ and $\Delta R_{\mu\gamma}$. The angular quantities η_γ and $\Delta R_{\mu\gamma}$ are themselves well measured. We use the iterative D’Agostini method of unfolding [22] as implemented in the ROOUNFOLD package [23]. By default, we unfold in the three quantities E_T , η_γ , and $\Delta R_{\mu\gamma}$ simultaneously after subtracting backgrounds; as a cross check we also unfold the E_T and $\Delta R_{\mu\gamma}$ distributions one at a time, and we also use a single-value decomposition method [24]. All results are consistent with each other. To verify the independence of the unfolded result on the assumed spectra, we distort the FSR model in an arbitrary manner when reconstructing the response matrix. The unfolded result is no different than the original one we obtained. A closure test in which the simulation is treated as data and undergoes the same unfolding procedure indicates no deviation greater than 1.5%.

The unfolding procedure corrects for the photon reconstruction and isolation efficiency. It also corrects for bias in the PF photon energy assuming that such a bias is reproduced in the simulation. Verification of the photon efficiencies and energy scale in data with respect to the simulation are discussed in Section 6.

6 Systematic uncertainties

Systematic uncertainties are assigned to each step of the analysis procedure using methods detailed in this section. Tables 3 and 4 present a summary of these uncertainties, which are

similar in magnitude to, or somewhat larger than the statistical uncertainties, depending on the photon E_T .

The muon efficiency, taken from simulation, is corrected as a function of p_T and η using a method derived from data and described in Ref. [17]. The statistical uncertainties for these corrections constitute a systematic uncertainty, which we also take from Ref. [17]. In addition, we assign a 0.5% uncertainty to account for the modifications of the standard isolation variable. We propagate the uncertainty in the muon efficiency by shifting the per-event weights up and down by one unit of systematic uncertainty.

The photon E_T scale is potentially an important source of systematic uncertainty although simulations indicate that the bias in PF photon energy is negligibly small. We verify the fidelity of the simulation by introducing an extra requirement, $0.05 < \Delta R_{\mu\gamma} \leq 0.9$, which gives us a high-purity subset of signal events in which the energy of the photon can be estimated from just the muon kinematics. We refer to this estimate as E_γ^{kin} . The quantity $s = 1 - (M_{\mu\mu\gamma}^2 - M_{\mu\mu}^2)/(M_Z^2 - M_{\mu\mu}^2) \approx 1 - E_\gamma^{\text{PF}}/E_\gamma^{\text{kin}}$ is distributed as a skewed Gaussian with a mean close to zero. We conducted detailed quantitative studies of the s distribution in bins of $E_{T\gamma}^{\text{PF}}$, separately in the barrel and endcaps. We fit the distributions to a Gaussian-like function in which the width parameter is itself a function of s , namely, $\sigma(s) = c(1 + e^{bs})$, with b and c as free parameters. Examples are given in Fig. 2. Overall, the simulation reproduces the s distributions in data very well. We derive some small corrections from the differences in data and simulation as a function of $E_{T\gamma}^{\text{PF}}$ and construct an alternate response matrix. The unfolded spectrum we obtained with this alternate response matrix differs from the original by less than 0.2% for $E_T < 40$ GeV, by less than 1% for $E_T < 75$ GeV, and by less than 3% in the highest E_T bin. We assign respective systematic uncertainties of 0.5%, 1%, and 3% for these three E_T ranges to account for the photon energy scale uncertainty.

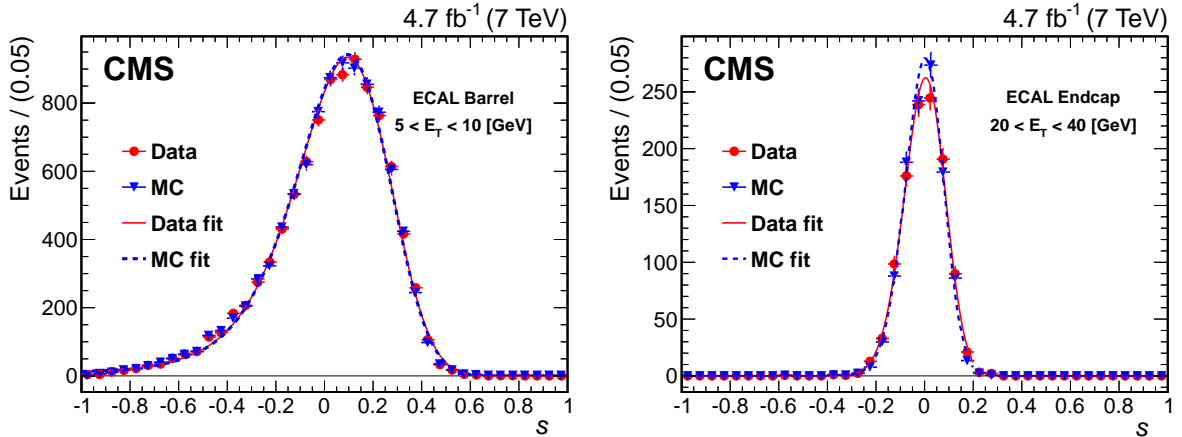


Figure 2: Two examples of an s distribution $s = 1 - (M_{\mu\mu\gamma}^2 - M_{\mu\mu}^2)/(M_Z^2 - M_{\mu\mu}^2)$ fit with a skewed Gaussian as described in the text. The left and right plots pertain to photons in the ECAL barrel with $5 < E_T < 10$ GeV and in the ECAL endcaps with $20 < E_T < 40$ GeV, respectively. The circle points and solid curve represent the data and the triangle points and dotted curve represent the simulation.

The photon energy resolution uncertainty is well constrained by studies with electrons and FSR photons [9]. To assess the impact of the uncertainty in the resolution, we degrade the photon energy resolution in simulated events by adding in quadrature a 1% term to the nominal resolution and construct a new response matrix. The differences in the unfolded spectrum relative to the default response matrix are small, and we take these differences as the systematic

Table 3: Relative systematic uncertainties for $d\sigma/dE_T$ (in percent).

Kinematic requirement [GeV]	Background estimation	Muon efficiency	Photon E_T -scale	Photon E_T resolution	Photon efficiency	Pileup photons	Unfolding	Total
$0.05 < \Delta R_{\mu\gamma} \leq 3$								
$5 < E_T \leq 10$	2.7	3.0	0.5	1.0	2.0	1.5	1.4	5.1
$10 < E_T \leq 15$	1.3	2.5	0.5	0.5	1.0	0.4	1.4	3.4
$15 < E_T \leq 20$	0.9	2.5	0.5	0.5	1.3	0.1	1.4	3.3
$20 < E_T \leq 25$	0.8	2.7	0.5	0.5	1.4	<0.1	1.4	3.5
$25 < E_T \leq 30$	0.7	3.3	0.5	0.5	1.5	<0.1	1.4	4.0
$30 < E_T \leq 40$	1.0	4.3	0.5	0.5	1.1	0.1	1.4	4.8
$40 < E_T \leq 50$	2.9	4.4	1.0	0.5	2.8	0.5	1.4	6.3
$50 < E_T \leq 75$	7.2	4.5	1.0	0.5	2.0	0.6	1.4	8.9
$75 < E_T \leq 100$	15.3	4.5	3.0	1.0	6.9	1.1	1.4	17.8
$0.05 < \Delta R_{\mu\gamma} \leq 0.5$								
$5 < E_T \leq 10$	0.8	2.1	0.5	1.0	2.0	0.1	1.4	3.5
$10 < E_T \leq 15$	0.4	2.0	0.5	0.5	1.0	<0.1	1.4	2.8
$15 < E_T \leq 20$	0.3	2.2	0.5	0.5	1.3	<0.1	1.4	3.1
$20 < E_T \leq 25$	0.3	2.5	0.5	0.5	1.4	<0.1	1.4	3.3
$25 < E_T \leq 30$	0.2	3.2	0.5	0.5	1.5	<0.1	1.4	3.9
$30 < E_T \leq 40$	0.3	4.3	0.5	0.5	1.1	<0.1	1.4	4.7
$40 < E_T \leq 50$	0.9	3.9	1.0	0.5	2.8	<0.1	1.4	5.2
$50 < E_T \leq 75$	2.3	3.0	1.0	0.5	2.0	<0.1	1.4	4.6
$75 < E_T \leq 100$	4.9	3.1	3.0	1.0	6.9	0.8	1.4	9.7
$0.5 < \Delta R_{\mu\gamma} \leq 3$								
$5 < E_T \leq 10$	6.4	4.7	0.5	1.0	2.0	3.8	1.4	9.2
$10 < E_T \leq 15$	2.8	3.2	0.5	0.5	1.0	0.8	1.4	4.7
$15 < E_T \leq 20$	1.9	2.8	0.5	0.5	1.3	0.3	1.4	4.0
$20 < E_T \leq 25$	1.7	3.0	0.5	0.5	1.4	<0.1	1.4	4.0
$25 < E_T \leq 30$	1.6	3.4	0.5	0.5	1.5	0.1	1.4	4.3
$30 < E_T \leq 40$	2.3	4.4	0.5	0.5	1.1	0.2	1.4	5.3
$40 < E_T \leq 50$	6.5	5.1	1.0	0.5	2.8	1.3	1.4	9.0
$50 < E_T \leq 75$	16.1	8.1	1.0	0.5	2.0	2.0	1.4	18.4
$75 < E_T \leq 100$	34.5	6.2	3.0	1.0	6.9	3.5	1.4	36.0
$0.05 < \Delta R_{\mu\gamma} \leq 3$ and $q_T < 10$ GeV								
$5 < E_T \leq 10$	1.4	2.2	0.5	1.0	2.0	1.0	1.4	3.9
$10 < E_T \leq 15$	0.6	1.9	0.5	0.5	1.0	0.1	1.4	2.8
$15 < E_T \leq 20$	0.4	2.1	0.5	0.5	1.3	<0.1	1.4	3.0
$20 < E_T \leq 25$	0.4	2.4	0.5	0.5	1.4	<0.1	1.4	3.3
$25 < E_T \leq 30$	0.5	3.5	0.5	0.5	1.5	<0.1	1.4	4.1
$30 < E_T \leq 40$	0.6	5.1	0.5	0.5	1.1	<0.1	1.4	5.5
$40 < E_T \leq 50$	7.3	4.7	1.0	0.5	2.8	1.0	1.4	9.4
$50 < E_T \leq 75$	18.2	8.5	1.0	0.5	2.0	4.4	1.4	20.8
$75 < E_T \leq 100$	38.9	6.4	3.0	1.0	6.9	<0.1	1.4	40.2
$0.05 < \Delta R_{\mu\gamma} \leq 3$ and $q_T > 50$ GeV								
$5 < E_T \leq 10$	5.7	4.2	0.5	1.0	2.0	1.8	1.4	7.8
$10 < E_T \leq 15$	3.0	3.3	0.5	0.5	1.0	0.4	1.4	4.9
$15 < E_T \leq 20$	3.0	2.8	0.5	0.5	1.3	0.3	1.4	4.6
$20 < E_T \leq 25$	2.3	2.7	0.5	0.5	1.4	0.2	1.4	4.2
$25 < E_T \leq 30$	1.9	2.6	0.5	0.5	1.5	0.1	1.4	3.9
$30 < E_T \leq 40$	2.9	2.9	0.5	0.5	1.1	0.3	1.4	4.6
$40 < E_T \leq 50$	1.5	2.8	1.0	0.5	2.8	0.2	1.4	4.6
$50 < E_T \leq 75$	3.9	2.8	1.0	0.5	2.0	0.3	1.4	5.5
$75 < E_T \leq 100$	8.2	3.5	3.0	1.0	6.9	0.2	1.4	11.8

Table 4: Relative systematic uncertainties for $d\sigma/d\Delta R_{\mu\gamma}$ (in percent).

Kinematic requirement	Background estimation	Muon efficiency	Photon E_T -scale	Photon resolution	Photon E_T efficiency	Pileup photons	Unfolding	Total
$E_T > 5.0 \text{ GeV}$								
$0.15 < \Delta R_{\mu\gamma} \leq 0.1$	0.7	2.4	<0.1	<0.1	1.0	<0.1	1.4	3.0
$0.1 < \Delta R_{\mu\gamma} \leq 0.15$	0.6	2.3	<0.1	<0.1	1.1	<0.1	1.4	3.0
$0.15 < \Delta R_{\mu\gamma} \leq 0.3$	0.4	2.3	<0.1	<0.1	1.0	<0.1	1.4	2.9
$0.3 < \Delta R_{\mu\gamma} \leq 0.5$	0.5	2.3	<0.1	<0.1	1.0	0.1	1.4	3.0
$0.5 < \Delta R_{\mu\gamma} \leq 0.8$	1.1	2.6	<0.1	<0.1	1.0	0.6	1.4	3.4
$0.8 < \Delta R_{\mu\gamma} \leq 1.2$	2.2	3.2	<0.1	<0.1	1.1	1.1	1.4	4.4
$1.2 < \Delta R_{\mu\gamma} \leq 1.6$	4.1	3.7	<0.1	<0.1	1.1	1.7	1.4	6.1
$1.6 < \Delta R_{\mu\gamma} \leq 2.0$	6.6	4.9	<0.1	<0.1	1.1	2.8	1.4	8.8
$2.0 < \Delta R_{\mu\gamma} \leq 3.0$	18.3	9.9	<0.1	<0.1	1.3	7.9	1.4	22.3
$E_T > 5.0 \text{ GeV and } q_T < 10 \text{ GeV}$								
$0.15 < \Delta R_{\mu\gamma} \leq 0.1$	0.2	2.1	<0.1	<0.1	1.0	<0.1	1.4	2.8
$0.1 < \Delta R_{\mu\gamma} \leq 0.15$	0.2	2.2	<0.1	<0.1	1.1	<0.1	1.4	2.8
$0.15 < \Delta R_{\mu\gamma} \leq 0.3$	0.1	2.1	<0.1	<0.1	1.0	<0.1	1.4	2.7
$0.3 < \Delta R_{\mu\gamma} \leq 0.5$	0.3	2.2	<0.1	<0.1	1.0	0.1	1.4	2.8
$0.5 < \Delta R_{\mu\gamma} \leq 0.8$	0.7	2.4	<0.1	<0.1	1.0	0.3	1.4	3.0
$0.8 < \Delta R_{\mu\gamma} \leq 1.2$	1.3	2.5	<0.1	<0.1	1.1	0.6	1.4	3.4
$1.2 < \Delta R_{\mu\gamma} \leq 1.6$	2.2	2.7	<0.1	<0.1	1.1	1.0	1.4	4.1
$1.6 < \Delta R_{\mu\gamma} \leq 2.0$	3.8	3.1	<0.1	<0.1	1.1	2.1	1.4	5.6
$2.0 < \Delta R_{\mu\gamma} \leq 3.0$	15.9	7.4	<0.1	<0.1	1.3	9.0	1.4	19.8
$E_T > 5.0 \text{ GeV and } q_T > 50 \text{ GeV}$								
$0.15 < \Delta R_{\mu\gamma} \leq 0.1$	1.8	2.5	<0.1	<0.1	1.0	<0.1	1.4	3.6
$0.1 < \Delta R_{\mu\gamma} \leq 0.15$	1.1	2.3	<0.1	<0.1	1.1	<0.1	1.4	3.1
$0.15 < \Delta R_{\mu\gamma} \leq 0.3$	1.5	2.4	<0.1	<0.1	1.0	<0.1	1.4	3.4
$0.3 < \Delta R_{\mu\gamma} \leq 0.5$	1.7	2.4	<0.1	<0.1	1.0	0.1	1.4	3.4
$0.5 < \Delta R_{\mu\gamma} \leq 0.8$	2.6	2.9	<0.1	<0.1	1.0	0.7	1.4	4.4
$0.8 < \Delta R_{\mu\gamma} \leq 1.2$	4.2	3.8	<0.1	<0.1	1.1	1.4	1.4	6.1
$1.2 < \Delta R_{\mu\gamma} \leq 1.6$	9.1	5.2	<0.1	<0.1	1.1	1.9	1.4	10.8
$1.6 < \Delta R_{\mu\gamma} \leq 2.0$	14.9	7.4	<0.1	<0.1	1.1	3.4	1.4	17.1
$2.0 < \Delta R_{\mu\gamma} \leq 3.0$	22.3	10.3	<0.1	<0.1	1.3	5.1	1.4	25.1

uncertainty due to photon energy resolution.

Efficiency corrections for photons are applied as part of the unfolding procedure described in Section 5 and are derived from the simulation. We verify these corrections using the data in the following way. An isolated FSR photon with $E_T > 5$ GeV nearly always produces a cluster in the ECAL. We define an efficiency to reconstruct and select PF photons given such isolated clusters. This efficiency rises from 60% for E_T between 5–10 GeV to approximately 90% for $E_T > 50$ GeV and is nearly the same in data and simulation. We take the difference, added in quadrature to the statistical uncertainties of the efficiencies, as the systematic uncertainty.

As described briefly in Section 5, the unfolding procedure has been cross-checked in several ways. To assess a systematic uncertainty due to unfolding, we use the small discrepancies observed in the closure test.

The uncertainty in the background estimate is dominated by the uncertainties associated with the corrections that we obtained from the control region (Section 4). The statistical uncertainty in the weights for jet multiplicity has a negligible impact, as does the correction for charged hadrons in the photon isolation cone. The parameterized functions to correct the photon distributions in E_T and η carry statistical uncertainties that we propagate to the measured cross sections through simplified MC models. Since the nonprompt photon E_T , η , and $\Delta R_{\mu\gamma}$ distributions in the control and signal regions are indistinguishable, we do not assess any uncertainty in the modeling.

The uncertainties in the non-DY backgrounds ($t\bar{t}$ and diboson production) are obtained from the uncertainties in the theoretical cross sections, the luminosity, and the statistical uncertainty in the simulated event samples. We assign 50% uncertainty to the W +jets and multijet background estimates, which are quite small.

The systematic uncertainty from the simulation of pileup depends primarily on the assumed cross section for additional pp collisions (roughly the same as the minimum-bias cross section) [25]. We vary the value of this cross section by 5% and evaluate the impact on the unfolded spectra.

The uncertainty in the integrated luminosity is 2.2% [26].

Theoretical uncertainties have been calculated and pertain to the reported theoretical prediction only. We propagated the uncertainty due to parton distribution functions (PDFs) using the prescription of Ref. [27]. We vary the factorization/renormalization scale parameters by a factor of 2 to estimate associated scale uncertainties introduced due to neglected higher-order quantum corrections. Finally, we include the MC statistical uncertainty.

7 Results

The differential cross sections are obtained by subtracting the estimated backgrounds from the observed distributions, unfolding the result, and dividing by the bin width and the integrated luminosity, $\mathcal{L} = 4.7 \text{ fb}^{-1}$. No acceptance correction is applied, so these cross sections are defined relative to the kinematic and fiducial requirements listed in Table 1.

The measured differential cross sections $d\sigma/dE_T$ and $d\sigma/d\Delta R_{\mu\gamma}$ are displayed in Fig. 3 and listed in Tables 5 and 6. A bin-centering correction is applied following the method of Ref. [28]; the abscissa of each point is based on the integral of the simulation across the bin and on the bin width. The shaded region represents the prediction and uncertainty from POWHEG+PYTHIA, obtained at the parton level: only the requirements in Table 1 have been applied to the generator-

level muons and photons. The agreement with data is good.

Energy spectra for photons closer to ($0.05 < \Delta R_{\mu\gamma} \leq 0.5$) and farther from the muon ($0.5 < \Delta R_{\mu\gamma} \leq 3$) are shown in Fig. 4. The rates for photons with large $\Delta R_{\mu\gamma}$ and E_T are also well reproduced. The number of events with $30 < M_{\mu\mu} < 87$ GeV is about 18% of the number with $60 < M_{\mu\mu} < 120$ GeV. Of the events with $30 < M_{\mu\mu} < 87$ GeV, the fraction of events with at least one photon with $E_T > 5$ GeV and $0.05 < \Delta R_{\mu\gamma} \leq 0.5$ is 8.7 ± 0.1 (stat) ± 0.2 (syst)%, and with $0.5 < \Delta R_{\mu\gamma} \leq 3$ is 5.6 ± 0.1 (stat) ± 0.2 (syst)%. Photons with $\Delta R_{\mu\gamma} > 1.2$ and $E_T > 40$ GeV constitute a small fraction $(1.3 \pm 0.5$ (stat) ± 0.6 (syst)) $\times 10^{-4}$.

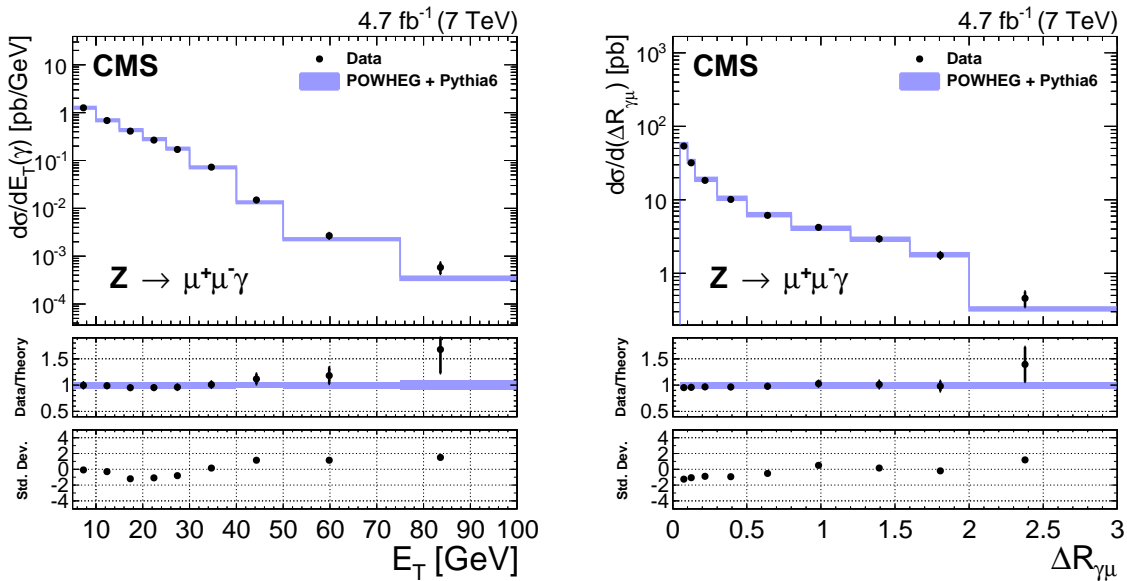


Figure 3: Measured differential cross sections $d\sigma/dE_T$ (left) and $d\sigma/d\Delta R_{\mu\gamma}$ (right). In the upper panels, the dots with error bars represent the data, and the shaded bands represent the POWHEG+PYTHIA calculation including theoretical uncertainties. The central panels display the ratio of data to the MC expectation. The lower panels show the standard deviations of the measurements with respect to the calculation. A bin-centering procedure has been applied.

We define two subsamples of signal events, one with the Z boson transverse momentum $q_T < 10$ GeV, and the other with $q_T > 50$ GeV. The measured cross sections shown in Fig. 5 demonstrate rather different energy spectra for these two cases, though $d\sigma/d\Delta R_{\mu\gamma}$ is basically the same.

As a final illustration of the nature of this event sample, we present distributions of dimuon mass ($M_{\mu\mu}$) and the three-body mass ($M_{\mu\mu\gamma}$) in Fig. 6. The small increase in the ratio of data to theory for $M_{\mu\mu} < 40$ GeV reflects the insufficient next-to-leading-order accuracy of the simulation; the kinematic requirements on the muons induce a loss of acceptance that require higher-order QCD corrections, as discussed in Ref. [17]. Although the masses of the dimuon pairs populate the tail of the Z resonance (in fact they were selected this way), the three-body mass distribution displays a nearly-symmetric resonance peak at the mass of the Z boson, thereby confirming the identity of these events as radiative decays $Z \rightarrow \mu^+ \mu^- \gamma$.

Table 5: Measured differential cross section $d\sigma/dE_T$ in pb/GeV. For the data values, the first uncertainty is statistical and the second is systematic. For the theory values, the uncertainty combines statistical, PDF, and renormalization/factorization scale components.

Kinematic requirement [GeV]	Data	POWHEG+PYTHIA
$0.05 < \Delta R_{\mu\gamma} \leq 3$		
$5 < E_T \leq 10$	$1.260 \pm 0.015 \pm 0.070$	1.270 ± 0.075
$10 < E_T \leq 15$	$0.685 \pm 0.009 \pm 0.028$	0.694 ± 0.040
$15 < E_T \leq 20$	$0.411 \pm 0.006 \pm 0.016$	0.433 ± 0.025
$20 < E_T \leq 25$	$0.267 \pm 0.005 \pm 0.011$	0.280 ± 0.017
$25 < E_T \leq 30$	$0.170 \pm 0.004 \pm 0.008$	0.177 ± 0.011
$30 < E_T \leq 40$	$(7.26 \pm 0.19 \pm 0.39) \times 10^{-2}$	$(7.20 \pm 0.42) \times 10^{-2}$
$40 < E_T \leq 50$	$(1.49 \pm 0.09 \pm 0.10) \times 10^{-2}$	$(1.34 \pm 0.08) \times 10^{-2}$
$50 < E_T \leq 75$	$(2.68 \pm 0.26 \pm 0.25) \times 10^{-3}$	$(2.27 \pm 0.14) \times 10^{-3}$
$75 < E_T \leq 100$	$(5.81 \pm 1.16 \pm 1.00) \times 10^{-4}$	$(3.47 \pm 0.32) \times 10^{-4}$
$0.05 < \Delta R_{\mu\gamma} \leq 0.5$		
$5 < E_T \leq 10$	$0.749 \pm 0.009 \pm 0.031$	0.779 ± 0.045
$10 < E_T \leq 15$	$0.417 \pm 0.006 \pm 0.015$	0.433 ± 0.025
$15 < E_T \leq 20$	$0.256 \pm 0.005 \pm 0.010$	0.272 ± 0.016
$20 < E_T \leq 25$	$0.168 \pm 0.004 \pm 0.007$	0.177 ± 0.011
$25 < E_T \leq 30$	$0.105 \pm 0.003 \pm 0.005$	0.112 ± 0.007
$30 < E_T \leq 40$	$(4.51 \pm 0.14 \pm 0.23) \times 10^{-2}$	$(4.44 \pm 0.26) \times 10^{-2}$
$40 < E_T \leq 50$	$(8.93 \pm 0.65 \pm 0.51) \times 10^{-3}$	$(8.53 \pm 0.50) \times 10^{-3}$
$50 < E_T \leq 75$	$(1.80 \pm 0.18 \pm 0.09) \times 10^{-3}$	$(1.63 \pm 0.10) \times 10^{-3}$
$75 < E_T \leq 100$	$(3.58 \pm 0.98 \pm 0.36) \times 10^{-4}$	$(2.42 \pm 0.37) \times 10^{-4}$
$0.5 < \Delta R_{\mu\gamma} \leq 3$		
$5 < E_T \leq 10$	$0.513 \pm 0.012 \pm 0.049$	0.489 ± 0.028
$10 < E_T \leq 15$	$0.268 \pm 0.006 \pm 0.014$	0.260 ± 0.015
$15 < E_T \leq 20$	$0.155 \pm 0.004 \pm 0.007$	0.161 ± 0.010
$20 < E_T \leq 25$	$(9.94 \pm 0.33 \pm 0.45) \times 10^{-2}$	$(1.03 \pm 0.06) \times 10^{-1}$
$25 < E_T \leq 30$	$(6.52 \pm 0.26 \pm 0.32) \times 10^{-2}$	$(6.55 \pm 0.39) \times 10^{-2}$
$30 < E_T \leq 40$	$(2.76 \pm 0.12 \pm 0.16) \times 10^{-2}$	$(2.76 \pm 0.17) \times 10^{-2}$
$40 < E_T \leq 50$	$(6.01 \pm 0.67 \pm 0.56) \times 10^{-3}$	$(4.85 \pm 0.33) \times 10^{-3}$
$50 < E_T \leq 75$	$(8.75 \pm 1.86 \pm 1.60) \times 10^{-4}$	$(6.38 \pm 0.60) \times 10^{-4}$
$75 < E_T \leq 100$	$(2.23 \pm 0.63 \pm 0.80) \times 10^{-4}$	$(1.04 \pm 0.27) \times 10^{-4}$
$0.05 < \Delta R_{\mu\gamma} \leq 3$ and $q_T < 10$ GeV		
$5 < E_T \leq 10$	$0.527 \pm 0.009 \pm 0.024$	0.535 ± 0.033
$10 < E_T \leq 15$	$0.294 \pm 0.005 \pm 0.010$	0.296 ± 0.018
$15 < E_T \leq 20$	$0.184 \pm 0.004 \pm 0.007$	0.191 ± 0.012
$20 < E_T \leq 25$	$0.127 \pm 0.003 \pm 0.005$	0.129 ± 0.008
$25 < E_T \leq 30$	$(8.59 \pm 0.28 \pm 0.40) \times 10^{-2}$	$(8.25 \pm 0.54) \times 10^{-2}$
$30 < E_T \leq 40$	$(3.22 \pm 0.12 \pm 0.19) \times 10^{-2}$	$(2.89 \pm 0.18) \times 10^{-2}$
$40 < E_T \leq 50$	$(1.46 \pm 0.27 \pm 0.14) \times 10^{-3}$	$(1.14 \pm 0.12) \times 10^{-3}$
$50 < E_T \leq 75$	$(1.92 \pm 0.67 \pm 0.42) \times 10^{-4}$	$(8.44 \pm 1.60) \times 10^{-5}$
$75 < E_T \leq 100$	$(1.67 \pm 2.10 \pm 0.66) \times 10^{-5}$	$(6.66 \pm 5.13) \times 10^{-6}$
$0.05 < \Delta R_{\mu\gamma} \leq 3$ and $q_T > 50$ GeV		
$5 < E_T \leq 10$	$0.104 \pm 0.005 \pm 0.008$	0.095 ± 0.005
$10 < E_T \leq 15$	$(6.26 \pm 0.28 \pm 0.33) \times 10^{-2}$	$(5.72 \pm 0.31) \times 10^{-2}$
$15 < E_T \leq 20$	$(3.67 \pm 0.20 \pm 0.19) \times 10^{-2}$	$(3.38 \pm 0.18) \times 10^{-2}$
$20 < E_T \leq 25$	$(2.19 \pm 0.15 \pm 0.10) \times 10^{-2}$	$(2.32 \pm 0.13) \times 10^{-2}$
$25 < E_T \leq 30$	$(1.94 \pm 0.14 \pm 0.09) \times 10^{-2}$	$(1.64 \pm 0.10) \times 10^{-2}$
$30 < E_T \leq 40$	$(9.98 \pm 0.71 \pm 0.51) \times 10^{-3}$	$(9.79 \pm 0.55) \times 10^{-3}$
$40 < E_T \leq 50$	$(6.21 \pm 0.55 \pm 0.32) \times 10^{-3}$	$(5.58 \pm 0.33) \times 10^{-3}$
$50 < E_T \leq 75$	$(1.90 \pm 0.20 \pm 0.11) \times 10^{-3}$	$(1.76 \pm 0.11) \times 10^{-3}$
$75 < E_T \leq 100$	$(4.56 \pm 0.95 \pm 0.55) \times 10^{-4}$	$(3.13 \pm 0.30) \times 10^{-4}$

Table 6: Measured differential cross section $d\sigma/d\Delta R_{\mu\gamma}$ in pb. For the data values, the first uncertainty is statistical and the second is systematic. For the theory values, the uncertainty combines statistical, PDF, and renormalization/factorization scale components.

Kinematic requirement	Data	POWHEG+PYTHIA
$E_T > 5.0 \text{ GeV}$		
$0.05 < \Delta R_{\mu\gamma} \leq 0.1$	$53.90 \pm 0.76 \pm 2.00$	56.60 ± 3.26
$0.1 < \Delta R_{\mu\gamma} \leq 0.15$	$31.90 \pm 0.59 \pm 1.20$	33.20 ± 1.96
$0.15 < \Delta R_{\mu\gamma} \leq 0.3$	$18.40 \pm 0.25 \pm 0.67$	19.00 ± 1.10
$0.3 < \Delta R_{\mu\gamma} \leq 0.5$	$10.10 \pm 0.16 \pm 0.37$	10.50 ± 0.59
$0.5 < \Delta R_{\mu\gamma} \leq 0.8$	$6.14 \pm 0.11 \pm 0.25$	6.29 ± 0.37
$0.8 < \Delta R_{\mu\gamma} \leq 1.2$	$4.22 \pm 0.09 \pm 0.21$	4.10 ± 0.24
$1.2 < \Delta R_{\mu\gamma} \leq 1.6$	$2.94 \pm 0.08 \pm 0.19$	2.91 ± 0.17
$1.6 < \Delta R_{\mu\gamma} \leq 2.0$	$1.76 \pm 0.07 \pm 0.16$	1.79 ± 0.11
$2.0 < \Delta R_{\mu\gamma} \leq 3.0$	$0.46 \pm 0.04 \pm 0.10$	0.33 ± 0.02
$E_T > \text{GeV and } q_T < 10 \text{ GeV}$		
$0.05 < \Delta R_{\mu\gamma} \leq 0.1$	$23.00 \pm 0.50 \pm 0.82$	24.40 ± 1.53
$0.1 < \Delta R_{\mu\gamma} \leq 0.15$	$13.70 \pm 0.39 \pm 0.49$	14.20 ± 0.88
$0.15 < \Delta R_{\mu\gamma} \leq 0.3$	$7.88 \pm 0.17 \pm 0.28$	8.21 ± 0.51
$0.3 < \Delta R_{\mu\gamma} \leq 0.5$	$4.38 \pm 0.10 \pm 0.16$	4.48 ± 0.28
$0.5 < \Delta R_{\mu\gamma} \leq 0.8$	$2.65 \pm 0.07 \pm 0.10$	2.67 ± 0.17
$0.8 < \Delta R_{\mu\gamma} \leq 1.2$	$1.75 \pm 0.05 \pm 0.07$	1.75 ± 0.11
$1.2 < \Delta R_{\mu\gamma} \leq 1.6$	$1.29 \pm 0.05 \pm 0.06$	1.25 ± 0.08
$1.6 < \Delta R_{\mu\gamma} \leq 2.0$	$0.72 \pm 0.04 \pm 0.04$	0.79 ± 0.05
$2.0 < \Delta R_{\mu\gamma} \leq 3.0$	$0.10 \pm 0.01 \pm 0.02$	0.09 ± 0.01
$E_T > 5.0 \text{ GeV and } q_T > 50 \text{ GeV}$		
$0.05 < \Delta R_{\mu\gamma} \leq 0.1$	$4.94 \pm 0.23 \pm 0.21$	5.07 ± 0.27
$0.1 < \Delta R_{\mu\gamma} \leq 0.15$	$2.97 \pm 0.18 \pm 0.11$	3.05 ± 0.18
$0.15 < \Delta R_{\mu\gamma} \leq 0.3$	$1.71 \pm 0.08 \pm 0.07$	1.73 ± 0.09
$0.3 < \Delta R_{\mu\gamma} \leq 0.5$	$0.95 \pm 0.05 \pm 0.04$	0.98 ± 0.06
$0.5 < \Delta R_{\mu\gamma} \leq 0.8$	$0.62 \pm 0.04 \pm 0.03$	0.58 ± 0.03
$0.8 < \Delta R_{\mu\gamma} \leq 1.2$	$0.44 \pm 0.03 \pm 0.03$	0.37 ± 0.02
$1.2 < \Delta R_{\mu\gamma} \leq 1.6$	$0.22 \pm 0.03 \pm 0.02$	0.19 ± 0.01
$1.6 < \Delta R_{\mu\gamma} \leq 2.0$	$0.13 \pm 0.02 \pm 0.02$	0.10 ± 0.01
$2.0 < \Delta R_{\mu\gamma} \leq 3.0$	$(8.45 \pm 1.38 \pm 2.10) \times 10^{-2}$	$(3.62 \pm 0.24) \times 10^{-2}$

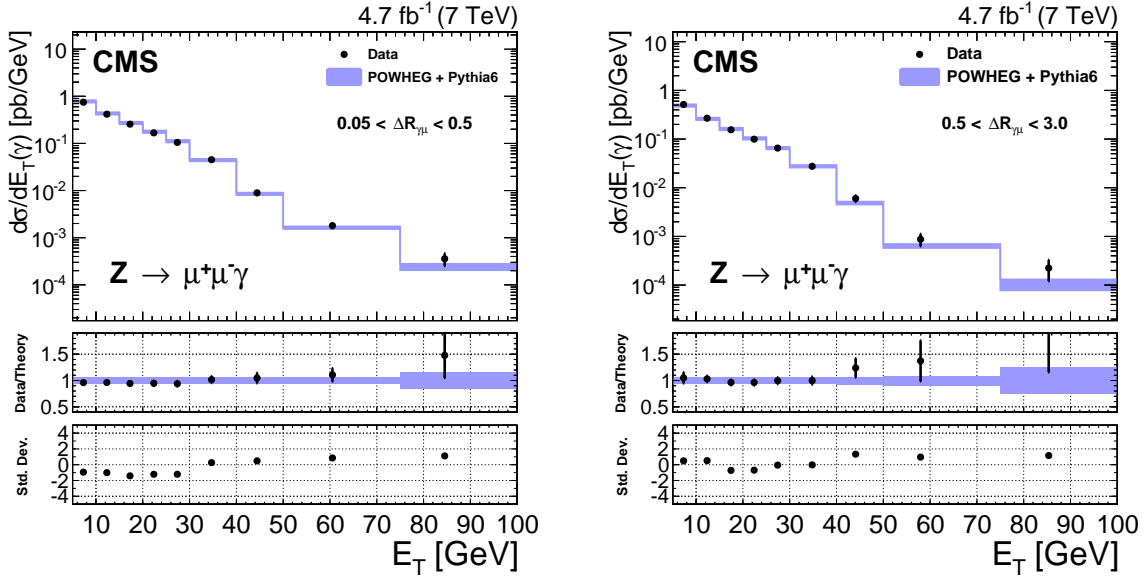


Figure 4: Measured differential cross sections $d\sigma/dE_T$ for photons close to the muon ($0.05 < \Delta R_{\mu\gamma} \leq 0.5$, left) and far from the muon ($0.5 < \Delta R_{\mu\gamma} \leq 3$, right). The dots with error bars represent the data, and the shaded bands represent the POWHEG+PYTHIA calculation including theoretical uncertainties. The central panels display the ratio of data to the MC expectation. The lower panels show the standard deviations of the measurements with respect to the calculation. A bin-centering procedure has been applied.

8 Summary

A study of final-state radiation in Z boson decays was presented. This study serves to test the simulation of events where mixed QED and QCD corrections are important. The analysis was performed on a sample of pp collision data at $\sqrt{s} = 7$ TeV recorded in 2011 with the CMS detector and corresponding to an integrated luminosity of 4.7 fb^{-1} . Events with two oppositely charged muons and an energetic, isolated photon were selected with only modest backgrounds. The differential cross sections $d\sigma/dE_T$ and $d\sigma/d\Delta R_{\mu\gamma}$ were measured for photons within the fiducial and kinematic requirements specified in Table 1, and comparisons of $d\sigma/dE_T$ for photons close to a muon and far from both muons were made. In addition, the differential cross sections $d\sigma/dE_T$ and $d\sigma/d\Delta R_{\mu\gamma}$ were compared for events with large and small transverse momentum of the Z boson, as computed from the two muons and the photon. Simulations based on POWHEG+PYTHIA reproduce the CMS data well, with discrepancies below 5% for $5 < E_T < 50 \text{ GeV}$ and $0.05 < \Delta R_{\mu\gamma} \leq 2$ as quantified in Tables 5 and 6.

Acknowledgments

We congratulate our colleagues in the CERN accelerator departments for the excellent performance of the LHC and thank the technical and administrative staffs at CERN and at other CMS institutes for their contributions to the success of the CMS effort. In addition, we gratefully acknowledge the computing centers and personnel of the Worldwide LHC Computing Grid for delivering so effectively the computing infrastructure essential to our analyses. Finally, we acknowledge the enduring support for the construction and operation of the LHC and the CMS detector provided by the following funding agencies: BMWFW and FWF (Austria); FNRS and

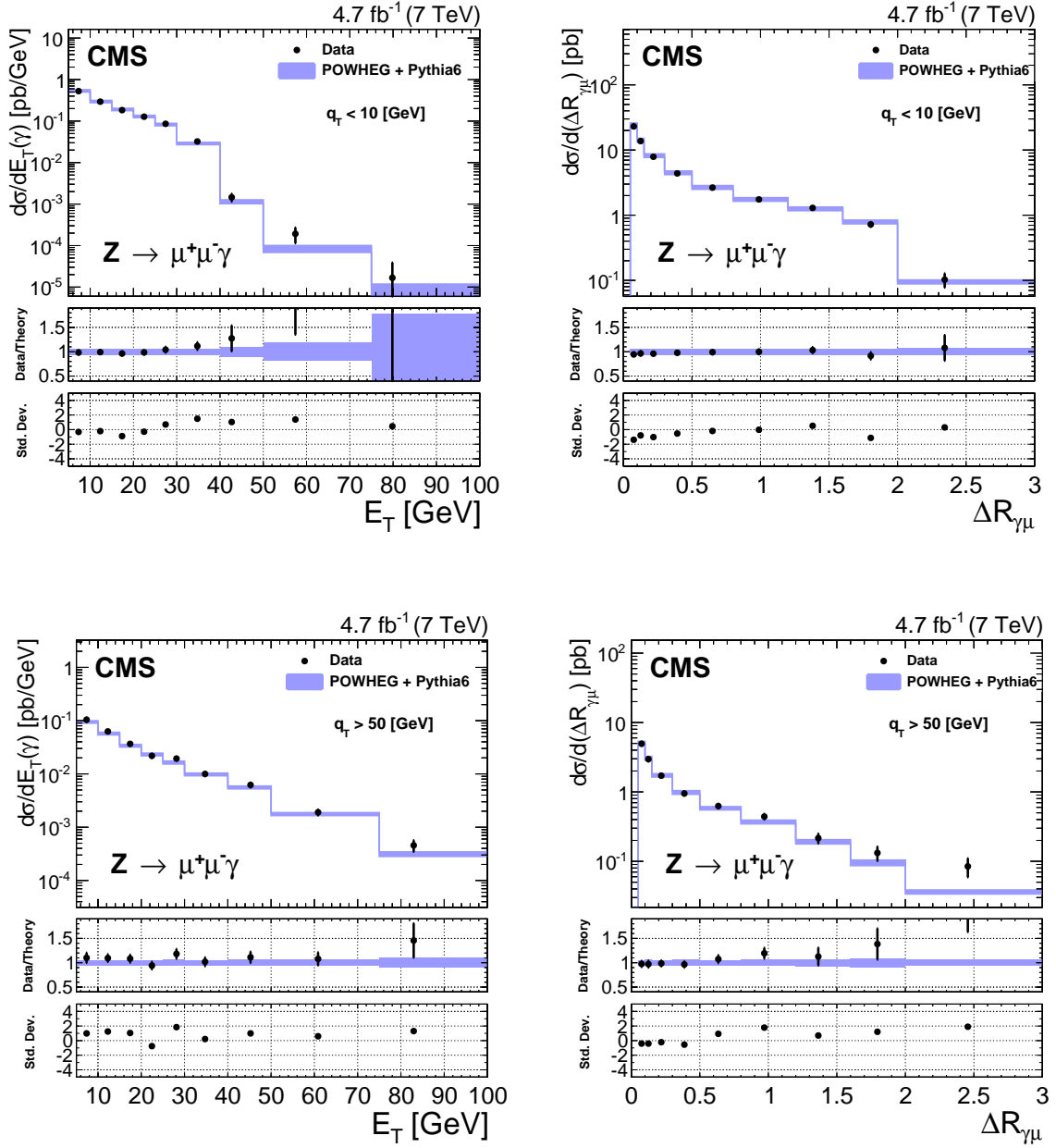


Figure 5: Measured differential cross sections $d\sigma/dE_T$ and $d\sigma/d\Delta R_{\mu\gamma}$ for $q_T < 10 \text{ GeV}$ (top row) and $q_T > 50 \text{ GeV}$ (bottom row). The dots with error bars represent the data, and the shaded bands represent the POWHEG+PYTHIA calculation including theoretical uncertainties. The central panels display the ratio of data to the MC expectation. The lower panels show the standard deviations of the measurements with respect to the calculation. A bin-centering procedure has been applied.

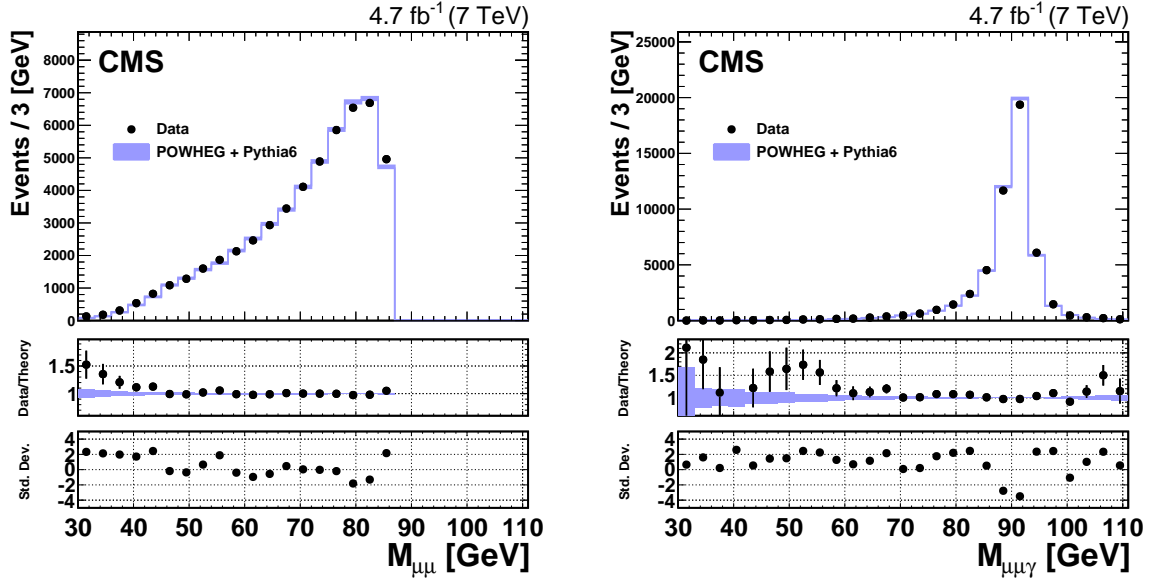


Figure 6: Distributions of the dimuon mass $M_{\mu\mu}$ (left) and the three-body mass $M_{\mu\mu\gamma}$ (right). The dots with error bars represent the data, and the shaded bands represent the POWHEG+PYTHIA prediction. The central panels display the ratio of data to the MC expectation. The lower panels show the standard deviations of the measurements with respect to the calculation. A bin-centering procedure has been applied.

FWO (Belgium); CNPq, CAPES, FAPERJ, and FAPESP (Brazil); MES (Bulgaria); CERN; CAS, MoST, and NSFC (China); COLCIENCIAS (Colombia); MSES and CSF (Croatia); RPF (Cyprus); MoER, ERC IUT and ERDF (Estonia); Academy of Finland, MEC, and HIP (Finland); CEA and CNRS/IN2P3 (France); BMBF, DFG, and HGF (Germany); GSRT (Greece); OTKA and NIH (Hungary); DAE and DST (India); IPM (Iran); SFI (Ireland); INFN (Italy); MSIP and NRF (Republic of Korea); LAS (Lithuania); MOE and UM (Malaysia); CINVESTAV, CONACYT, SEP, and UASLP-FAI (Mexico); MBIE (New Zealand); PAEC (Pakistan); MSHE and NSC (Poland); FCT (Portugal); JINR (Dubna); MON, RosAtom, RAS and RFBR (Russia); MESTD (Serbia); SEIDI and CPAN (Spain); Swiss Funding Agencies (Switzerland); MST (Taipei); ThEPCenter, IPST, STAR and NSTDA (Thailand); TUBITAK and TAEK (Turkey); NASU and SFFR (Ukraine); STFC (United Kingdom); DOE and NSF (USA).

Individuals have received support from the Marie-Curie program and the European Research Council and EPLANET (European Union); the Leventis Foundation; the A. P. Sloan Foundation; the Alexander von Humboldt Foundation; the Belgian Federal Science Policy Office; the Fonds pour la Formation à la Recherche dans l'Industrie et dans l'Agriculture (FRIA-Belgium); the Agentschap voor Innovatie door Wetenschap en Technologie (IWT-Belgium); the Ministry of Education, Youth and Sports (MEYS) of the Czech Republic; the Council of Science and Industrial Research, India; the HOMING PLUS program of Foundation for Polish Science, cofinanced from European Union, Regional Development Fund; the Compagnia di San Paolo (Torino); the Consorzio per la Fisica (Trieste); MIUR project 20108T4XTM (Italy); the Thalís and Aristeia programs cofinanced by EU-ESF and the Greek NSRF; and the National Priorities Research Program by Qatar National Research Fund.

References

- [1] UA1 Collaboration, “Studies of intermediate vector boson production and decay in UA1 at the CERN proton-antiproton collider”, *Z. Phys. C* **44** (1989) 15, doi:10.1007/BF01548582.
- [2] UA2 Collaboration, “Evidence for $Z^0 \rightarrow e^+e^-$ at the CERN $\bar{p}p$ collider”, *Phys. Lett. B* **129** (1983) 130, doi:10.1016/0370-2693(83)90744-X.
- [3] Y. Li and F. Petriello, “Combining QCD and electroweak corrections to dilepton production in the framework of the FEWZ simulation code”, *Phys. Rev. D* **86** (2012) 094034, doi:10.1103/PhysRevD.86.094034, arXiv:1208.5967.
- [4] S. Dittmaier, A. Huss, and C. Schwinn, “ $O(\alpha_s\alpha)$ corrections to Drell-Yan processes in the resonance region”, *PoS LL2014* (2014) 045, arXiv:1405.6897.
- [5] C. Bernaciak and D. Wackerth, “Combining NLO QCD and electroweak radiative corrections to W boson production at hadron colliders in the POWHEG framework”, *Phys. Rev. D* **85** (2012) 093003, doi:10.1103/PhysRevD.85.093003, arXiv:1201.4804.
- [6] L. Barze et al., “Implementation of electroweak corrections in the POWHEG BOX: single W production”, *JHEP* **04** (2012) 037, doi:10.1007/JHEP04(2012)037, arXiv:1202.0465.
- [7] CMS Collaboration, “The CMS experiment at the CERN LHC”, *JINST* **3** (2008) S08004, doi:10.1088/1748-0221/3/08/S08004.
- [8] CMS Collaboration, “Performance of CMS muon reconstruction in pp collision events at $\sqrt{s} = 7$ TeV”, *JINST* **7** (2012) P10002, doi:10.1088/1748-0221/7/10/P10002, arXiv:1206.4071.
- [9] CMS Collaboration, “Energy calibration and resolution of the CMS electromagnetic calorimeter in pp collisions at $\sqrt{s} = 7$ TeV”, *JINST* **8** (2013) P09009, doi:10.1088/1748-0221/8/09/P09009, arXiv:1306.2016.
- [10] CMS Collaboration, “The CMS TriDAS Project: Technical Design Report, Volume 1: The Trigger System”, CMS TDR CERN/LHCC 2000-038, 2000.
- [11] CMS Collaboration, “The TriDAS Project: Technical Design Report, Volume 2: Data acquisition and high-level trigger”, CMS TDR CERN/LHCC 2002-026, 2002.
- [12] S. Alioli, P. Nason, C. Oleari, and E. Re, “NLO vector-boson production matched with shower in POWHEG”, *JHEP* **07** (2008) 060, doi:10.1088/1126-6708/2008/07/060, arXiv:0805.4802.
- [13] T. Sjöstrand, S. Mrenna, and P. Skands, “PYTHIA 6.4 physics and manual”, *JHEP* **05** (2006) 026, doi:10.1088/1126-6708/2006/05/026, arXiv:hep-ph/0603175.
- [14] H.-L. Lai et al., “New parton distributions for collider physics”, *Phys. Rev. D* **82** (2010) 074024, doi:10.1103/PhysRevD.82.074024, arXiv:1007.2241.
- [15] R. Field, “Min-bias and the underlying event at the LHC”, *Acta Phys. Polon. B* **42** (2011) 2631, doi:10.5506/APhysPolB.42.2631, arXiv:1202.0901.

- [16] GEANT4 Collaboration, "GEANT4—a simulation toolkit", *Nucl. Instrum. Meth. A* **506** (2003) 250, doi:10.1016/S0168-9002(03)01368-8.
- [17] CMS Collaboration, "Measurement of the Drell-Yan cross section in pp collisions at $\sqrt{s} = 7$ TeV", *JHEP* **10** (2011) 007, doi:10.1007/JHEP10(2011)007, arXiv:1108.0566.
- [18] CMS Collaboration, "Commissioning of the Particle-flow Event Reconstruction with the first LHC collisions recorded in the CMS detector", CMS Physics Analysis Summary CMS-PAS-PFT-10-001, 2010.
- [19] CMS Collaboration, "Particle-Flow event reconstruction in CMS and performance for jets, taus, and MET", CMS Physics Analysis Summary CMS-PAS-PFT-09-001, 2009.
- [20] M. Cacciari, G. P. Salam, and G. Soyez, "The anti- k_t jet clustering algorithm", *JHEP* **04** (2008) 063, doi:10.1088/1126-6708/2008/04/063, arXiv:0802.1189.
- [21] A. Bodek et al., "Extracting muon momentum scale corrections for hadron collider experiments", *Eur. Phys. J. C* **72** (2012) 2194, doi:10.1140/epjc/s10052-012-2194-8, arXiv:1208.3710.
- [22] G. D'Agostini, "A multidimensional unfolding method based on Bayes' theorem", *Nucl. Instrum. Meth. A* **362** (1995) 487, doi:10.1016/0168-9002(95)00274-X.
- [23] T. Auye, "Unfolding algorithms and tests using RooUnfold", in *PHYSTAT 2011 Workshop on Statistical Issues Related to Discovery Claims in Search Experiments and Unfolding*, H. Prosper and L. Lyons, eds., p. 313. Geneva, Switzerland, 2011. arXiv:1105.1160. doi:10.5170/CERN-2011-006.313.
- [24] A. Höcker and V. Kartvelishvili, "SVD approach to data unfolding", *Nucl. Instrum. Meth. A* **372** (1996) 469, doi:10.1016/0168-9002(95)01478-0, arXiv:hep-ph/9509307.
- [25] CMS Collaboration, "Measurement of the inelastic proton-proton cross section at $\sqrt{s} = 7$ TeV", *Phys. Lett. B* **722** (2013) 5, doi:10.1016/j.physletb.2013.03.024, arXiv:1210.6718.
- [26] CMS Collaboration, "Absolute Calibration of the Luminosity Measurement at CMS: Winter 2012 Update", CMS Physics Analysis Summary CMS-PAS-SMP-12-008, 2012.
- [27] M. R. Whalley, D. Bourilkov, and R. C. Group, "The Les Houches Accord PDFs (LHAPDF) and Lhaglu", (2005). arXiv:hep-ph/0508110.
- [28] G. D. Lafferty and T. R. Wyatt, "Where to stick your data points: The treatment of measurements within wide bins", *Nucl. Instrum. Meth. A* **355** (1995) 541, doi:10.1016/0168-9002(94)01112-5.

A The CMS Collaboration

Yerevan Physics Institute, Yerevan, Armenia

V. Khachatryan, A.M. Sirunyan, A. Tumasyan

Institut für Hochenergiephysik der OeAW, Wien, Austria

W. Adam, T. Bergauer, M. Dragicevic, J. Erö, M. Friedl, R. Frühwirth¹, V.M. Ghete, C. Hartl, N. Hörmann, J. Hrubec, M. Jeitler¹, W. Kiesenhofer, V. Knünz, M. Krammer¹, I. Krätschmer, D. Liko, I. Mikulec, D. Rabadý², B. Rahbaran, H. Rohringer, R. Schöfbeck, J. Strauss, W. Treberer-Treberspurg, W. Waltenberger, C.-E. Wulz¹

National Centre for Particle and High Energy Physics, Minsk, Belarus

V. Mossolov, N. Shumeiko, J. Suarez Gonzalez

Universiteit Antwerpen, Antwerpen, Belgium

S. Alderweireldt, S. Bansal, T. Cornelis, E.A. De Wolf, X. Janssen, A. Knutsson, J. Lauwers, S. Luyckx, S. Ochesanu, R. Rougny, M. Van De Klundert, H. Van Haeveermaet, P. Van Mechelen, N. Van Remortel, A. Van Spilbeeck

Vrije Universiteit Brussel, Brussel, Belgium

F. Blekman, S. Blyweert, J. D'Hondt, N. Daci, N. Heracleous, J. Keaveney, S. Lowette, M. Maes, A. Olbrechts, Q. Python, D. Strom, S. Tavernier, W. Van Doninck, P. Van Mulders, G.P. Van Onsem, I. Vilella

Université Libre de Bruxelles, Bruxelles, Belgium

C. Caillol, B. Clerbaux, G. De Lentdecker, D. Dobur, L. Favart, A.P.R. Gay, A. Grebenyuk, A. Léonard, A. Mohammadi, L. Perniè², A. Randle-conde, T. Reis, T. Seva, L. Thomas, C. Vander Velde, P. Vanlaer, J. Wang, F. Zenoni

Ghent University, Ghent, Belgium

V. Adler, K. Beernaert, L. Benucci, A. Cimmino, S. Costantini, S. Crucy, A. Fagot, G. Garcia, J. Mccartin, A.A. Ocampo Rios, D. Poyraz, D. Ryckbosch, S. Salva Diblen, M. Sigamani, N. Strobbe, F. Thyssen, M. Tytgat, E. Yazgan, N. Zaganidis

Université Catholique de Louvain, Louvain-la-Neuve, Belgium

S. Basegmez, C. Beluffi³, G. Bruno, R. Castello, A. Caudron, L. Ceard, G.G. Da Silveira, C. Delaere, T. du Pree, D. Favart, L. Forthomme, A. Giammanco⁴, J. Hollar, A. Jafari, P. Jez, M. Komm, V. Lemaitre, C. Nuttens, L. Perrini, A. Pin, K. Piotrkowski, A. Popov⁵, L. Quertenmont, M. Selvaggi, M. Vidal Marono, J.M. Vizan Garcia

Université de Mons, Mons, Belgium

N. Bely, T. Caebergs, E. Daubie, G.H. Hammad

Centro Brasileiro de Pesquisas Fisicas, Rio de Janeiro, Brazil

W.L. Aldá Júnior, G.A. Alves, L. Brito, M. Correa Martins Junior, T. Dos Reis Martins, J. Molina, C. Mora Herrera, M.E. Pol, P. Rebello Teles

Universidade do Estado do Rio de Janeiro, Rio de Janeiro, Brazil

W. Carvalho, J. Chinellato⁶, A. Custódio, E.M. Da Costa, D. De Jesus Damiao, C. De Oliveira Martins, S. Fonseca De Souza, H. Malbouisson, D. Matos Figueiredo, L. Mundim, H. Nogima, W.L. Prado Da Silva, J. Santaolalla, A. Santoro, A. Sznajder, E.J. Tonelli Manganote⁶, A. Vilela Pereira

Universidade Estadual Paulista ^a, Universidade Federal do ABC ^b, São Paulo, Brazil

C.A. Bernardes^b, S. Dogra^a, T.R. Fernandez Perez Tomei^a, E.M. Gregores^b, P.G. Mercadante^b, S.F. Novaes^a, Sandra S. Padula^a

Institute for Nuclear Research and Nuclear Energy, Sofia, Bulgaria

A. Aleksandrov, V. Genchev², R. Hadjiiska, P. Iaydjiev, A. Marinov, S. Piperov, M. Rodozov, S. Stoykova, G. Sultanov, M. Vutova

University of Sofia, Sofia, Bulgaria

A. Dimitrov, I. Glushkov, L. Litov, B. Pavlov, P. Petkov

Institute of High Energy Physics, Beijing, China

J.G. Bian, G.M. Chen, H.S. Chen, M. Chen, T. Cheng, R. Du, C.H. Jiang, R. Plestina⁷, F. Romeo, J. Tao, Z. Wang

State Key Laboratory of Nuclear Physics and Technology, Peking University, Beijing, China

C. Asawatrangkuldee, Y. Ban, S. Liu, Y. Mao, S.J. Qian, D. Wang, Z. Xu, L. Zhang, W. Zou

Universidad de Los Andes, Bogota, Colombia

C. Avila, A. Cabrera, L.F. Chaparro Sierra, C. Florez, J.P. Gomez, B. Gomez Moreno, J.C. Sanabria

University of Split, Faculty of Electrical Engineering, Mechanical Engineering and Naval Architecture, Split, Croatia

N. Godinovic, D. Lelas, D. Polic, I. Puljak

University of Split, Faculty of Science, Split, Croatia

Z. Antunovic, M. Kovac

Institute Rudjer Boskovic, Zagreb, Croatia

V. Brigljevic, K. Kadija, J. Luetic, D. Mekterovic, L. Sudic

University of Cyprus, Nicosia, Cyprus

A. Attikis, G. Mavromanolakis, J. Mousa, C. Nicolaou, F. Ptochos, P.A. Razis, H. Rykaczewski

Charles University, Prague, Czech Republic

M. Bodlak, M. Finger, M. Finger Jr.⁸

Academy of Scientific Research and Technology of the Arab Republic of Egypt, Egyptian Network of High Energy Physics, Cairo, Egypt

Y. Assran⁹, A. Ellithi Kamel¹⁰, M.A. Mahmoud¹¹, A. Radi^{12,13}

National Institute of Chemical Physics and Biophysics, Tallinn, Estonia

M. Kadastik, M. Murumaa, M. Raidal, A. Tiko

Department of Physics, University of Helsinki, Helsinki, Finland

P. Eerola, M. Voutilainen

Helsinki Institute of Physics, Helsinki, Finland

J. Härkönen, V. Karimäki, R. Kinnunen, M.J. Kortelainen, T. Lampén, K. Lassila-Perini, S. Lehti, T. Lindén, P. Luukka, T. Mäenpää, T. Peltola, E. Tuominen, J. Tuominiemi, E. Tuovinen, L. Wendland

Lappeenranta University of Technology, Lappeenranta, Finland

J. Talvitie, T. Tuuva

DSM/IRFU, CEA/Saclay, Gif-sur-Yvette, France

M. Besancon, F. Couderc, M. Dejardin, D. Denegri, B. Fabbro, J.L. Faure, C. Favaro, F. Ferri, S. Ganjour, A. Givernaud, P. Gras, G. Hamel de Monchenault, P. Jarry, E. Locci, J. Malcles, J. Rander, A. Rosowsky, M. Titov

Laboratoire Leprince-Ringuet, Ecole Polytechnique, IN2P3-CNRS, Palaiseau, France

S. Baffioni, F. Beaudette, P. Busson, E. Chapon, C. Charlot, T. Dahms, M. Dalchenko, L. Dobrzynski, N. Filipovic, A. Florent, R. Granier de Cassagnac, L. Mastrolorenzo, P. Miné, I.N. Naranjo, M. Nguyen, C. Ochando, G. Ortona, P. Paganini, S. Regnard, R. Salerno, J.B. Sauvan, Y. Sirois, C. Veelken, Y. Yilmaz, A. Zabi

Institut Pluridisciplinaire Hubert Curien, Université de Strasbourg, Université de Haute Alsace Mulhouse, CNRS/IN2P3, Strasbourg, France

J.-L. Agram¹⁴, J. Andrea, A. Aubin, D. Bloch, J.-M. Brom, E.C. Chabert, C. Collard, E. Conte¹⁴, J.-C. Fontaine¹⁴, D. Gelé, U. Goerlach, C. Goetzmann, A.-C. Le Bihan, K. Skovpen, P. Van Hove

Centre de Calcul de l'Institut National de Physique Nucleaire et de Physique des Particules, CNRS/IN2P3, Villeurbanne, France

S. Gadrat

Université de Lyon, Université Claude Bernard Lyon 1, CNRS-IN2P3, Institut de Physique Nucléaire de Lyon, Villeurbanne, France

S. Beauceron, N. Beaupere, C. Bernet⁷, G. Boudoul², E. Bouvier, S. Brochet, C.A. Carrillo Montoya, J. Chasserat, R. Chierici, D. Contardo², B. Courbon, P. Depasse, H. El Mamouni, J. Fan, J. Fay, S. Gascon, M. Gouzevitch, B. Ille, T. Kurca, M. Lethuillier, L. Mirabito, A.L. Pequegnot, S. Perries, J.D. Ruiz Alvarez, D. Sabes, L. Sgandurra, V. Sordini, M. Vander Donckt, P. Verdier, S. Viret, H. Xiao

Institute of High Energy Physics and Informatization, Tbilisi State University, Tbilisi, Georgia

Z. Tsamalaidze⁸

RWTH Aachen University, I. Physikalisches Institut, Aachen, Germany

C. Autermann, S. Beranek, M. Bontenackels, M. Edelhoff, L. Feld, A. Heister, K. Klein, M. Lipinski, A. Ostapchuk, M. Preuten, F. Raupach, J. Sammet, S. Schael, J.F. Schulte, H. Weber, B. Wittmer, V. Zhukov⁵

RWTH Aachen University, III. Physikalisches Institut A, Aachen, Germany

M. Ata, M. Brodski, E. Dietz-Laursonn, D. Duchardt, M. Erdmann, R. Fischer, A. Güth, T. Hebbeker, C. Heidemann, K. Hoepfner, D. Klingebiel, S. Knutzen, P. Kreuzer, M. Merschmeyer, A. Meyer, P. Millet, M. Olschewski, K. Padeken, P. Papacz, H. Reithler, S.A. Schmitz, L. Sonnenschein, D. Teyssier, S. Thüer

RWTH Aachen University, III. Physikalisches Institut B, Aachen, Germany

V. Cherepanov, Y. Erdogan, G. Flügge, H. Geenen, M. Geisler, W. Haj Ahmad, F. Hoehle, B. Kargoll, T. Kress, Y. Kuessel, A. Künsken, J. Lingemann², A. Nowack, I.M. Nugent, C. Pistone, O. Pooth, A. Stahl

Deutsches Elektronen-Synchrotron, Hamburg, Germany

M. Aldaya Martin, I. Asin, N. Bartosik, J. Behr, U. Behrens, A.J. Bell, A. Bethani, K. Borras, A. Burgmeier, A. Cakir, L. Calligaris, A. Campbell, S. Choudhury, F. Costanza, C. Diez Pardos, G. Dolinska, S. Dooling, T. Dorland, G. Eckerlin, D. Eckstein, T. Eichhorn, G. Flucke, J. Garay Garcia, A. Geiser, A. Gizhko, P. Gunnellini, J. Hauk, M. Hempel¹⁵, H. Jung, A. Kalogeropoulos, O. Karacheban¹⁵, M. Kasemann, P. Katsas, J. Kieseler, C. Kleinwort, I. Korol,

D. Krücker, W. Lange, J. Leonard, K. Lipka, A. Lobanov, W. Lohmann¹⁵, B. Lutz, R. Mankel, I. Marfin¹⁵, I.-A. Melzer-Pellmann, A.B. Meyer, G. Mittag, J. Mnich, A. Mussgiller, S. Naumann-Emme, A. Nayak, E. Ntomari, H. Perrey, D. Pitzl, R. Placakyte, A. Raspereza, P.M. Ribeiro Cipriano, B. Roland, E. Ron, M.Ö. Sahin, J. Salfeld-Nebgen, P. Saxena, T. Schoerner-Sadenius, M. Schröder, C. Seitz, S. Spannagel, A.D.R. Vargas Trevino, R. Walsh, C. Wissing

University of Hamburg, Hamburg, Germany

V. Blobel, M. Centis Vignali, A.R. Draeger, J. Erfle, E. Garutti, K. Goebel, M. Görner, J. Haller, M. Hoffmann, R.S. Höing, A. Junkes, H. Kirschenmann, R. Klanner, R. Kogler, T. Lapsien, T. Lenz, I. Marchesini, D. Marconi, J. Ott, T. Peiffer, A. Perieanu, N. Pietsch, J. Poehlsen, T. Poehlsen, D. Rathjens, C. Sander, H. Schettler, P. Schleper, E. Schlieckau, A. Schmidt, M. Seidel, V. Sola, H. Stadie, G. Steinbrück, D. Troendle, E. Usai, L. Vanelderen, A. Vanhoefer

Institut für Experimentelle Kernphysik, Karlsruhe, Germany

C. Barth, C. Baus, J. Berger, C. Böser, E. Butz, T. Chwalek, W. De Boer, A. Descroix, A. Dierlamm, M. Feindt, F. Frensch, M. Giffels, A. Gilbert, F. Hartmann², T. Hauth, U. Husemann, I. Katkov⁵, A. Kornmayer², P. Lobelle Pardo, M.U. Mozer, T. Müller, Th. Müller, A. Nürnberg, G. Quast, K. Rabbertz, S. Röcker, H.J. Simonis, F.M. Stober, R. Ulrich, J. Wagner-Kuhr, S. Wayand, T. Weiler, R. Wolf

Institute of Nuclear and Particle Physics (INPP), NCSR Demokritos, Aghia Paraskevi, Greece

G. Anagnostou, G. Daskalakis, T. Gerasis, V.A. Giakoumopoulou, A. Kyriakis, D. Loukas, A. Markou, C. Markou, A. Psallidas, I. Topsis-Giotis

University of Athens, Athens, Greece

A. Agapitos, S. Kesisoglou, A. Panagiotou, N. Saoulidou, E. Stiliaris, E. Tziaferi

University of Ioánnina, Ioánnina, Greece

X. Aslanoglou, I. Evangelou, G. Flouris, C. Foudas, P. Kokkas, N. Manthos, I. Papadopoulos, E. Paradas, J. Strologas

Wigner Research Centre for Physics, Budapest, Hungary

G. Bencze, C. Hajdu, P. Hidas, D. Horvath¹⁶, F. Sikler, V. Veszpremi, G. Vesztergombi¹⁷, A.J. Zsigmond

Institute of Nuclear Research ATOMKI, Debrecen, Hungary

N. Beni, S. Czellar, J. Karancsi¹⁸, J. Molnar, J. Palinkas, Z. Szillasi

University of Debrecen, Debrecen, Hungary

A. Makovec, P. Raics, Z.L. Trocsanyi, B. Ujvari

National Institute of Science Education and Research, Bhubaneswar, India

S.K. Swain

Panjab University, Chandigarh, India

S.B. Beri, V. Bhatnagar, R. Gupta, U. Bhawandeep, A.K. Kalsi, M. Kaur, R. Kumar, M. Mittal, N. Nishu, J.B. Singh

University of Delhi, Delhi, India

Ashok Kumar, Arun Kumar, S. Ahuja, A. Bhardwaj, B.C. Choudhary, A. Kumar, S. Malhotra, M. Naimuddin, K. Ranjan, V. Sharma

Saha Institute of Nuclear Physics, Kolkata, India

S. Banerjee, S. Bhattacharya, K. Chatterjee, S. Dutta, B. Gomber, Sa. Jain, Sh. Jain, R. Khurana, A. Modak, S. Mukherjee, D. Roy, S. Sarkar, M. Sharan

Bhabha Atomic Research Centre, Mumbai, India

A. Abdulsalam, D. Dutta, V. Kumar, A.K. Mohanty², L.M. Pant, P. Shukla, A. Topkar

Tata Institute of Fundamental Research, Mumbai, India

T. Aziz, S. Banerjee, S. Bhowmik¹⁹, R.M. Chatterjee, R.K. Dewanjee, S. Dugad, S. Ganguly, S. Ghosh, M. Guchait, A. Gurtu²⁰, G. Kole, S. Kumar, M. Maity¹⁹, G. Majumder, K. Mazumdar, G.B. Mohanty, B. Parida, K. Sudhakar, N. Wickramage²¹

Indian Institute of Science Education and Research (IISER), Pune, India

S. Sharma

Institute for Research in Fundamental Sciences (IPM), Tehran, Iran

H. Bakhshiansohi, H. Behnamian, S.M. Etesami²², A. Fahim²³, R. Goldouzian, M. Khakzad, M. Mohammadi Najafabadi, M. Naseri, S. Paktinat Mehdiabadi, F. Rezaei Hosseinabadi, B. Safarzadeh²⁴, M. Zeinali

University College Dublin, Dublin, Ireland

M. Felcini, M. Grunewald

INFN Sezione di Bari ^a, Università di Bari ^b, Politecnico di Bari ^c, Bari, Italy

M. Abbrescia^{a,b}, C. Calabria^{a,b}, S.S. Chhibra^{a,b}, A. Colaleo^a, D. Creanza^{a,c}, L. Cristella^{a,b}, N. De Filippis^{a,c}, M. De Palma^{a,b}, L. Fiore^a, G. Iaselli^{a,c}, G. Maggi^{a,c}, M. Maggi^a, S. My^{a,c}, S. Nuzzo^{a,b}, A. Pompili^{a,b}, G. Pugliese^{a,c}, R. Radogna^{a,b,2}, G. Selvaggi^{a,b}, A. Sharma^a, L. Silvestris^{a,2}, R. Venditti^{a,b}, P. Verwilligen^a

INFN Sezione di Bologna ^a, Università di Bologna ^b, Bologna, Italy

G. Abbiendi^a, A.C. Benvenuti^a, D. Bonacorsi^{a,b}, S. Braibant-Giacomelli^{a,b}, L. Brigliadori^{a,b}, R. Campanini^{a,b}, P. Capiluppi^{a,b}, A. Castro^{a,b}, F.R. Cavallo^a, G. Codispoti^{a,b}, M. Cuffiani^{a,b}, G.M. Dallavalle^a, F. Fabbri^a, A. Fanfani^{a,b}, D. Fasanella^{a,b}, P. Giacomelli^a, C. Grandi^a, L. Guiducci^{a,b}, S. Marcellini^a, G. Masetti^a, A. Montanari^a, F.L. Navarria^{a,b}, A. Perrotta^a, A.M. Rossi^{a,b}, T. Rovelli^{a,b}, G.P. Siroli^{a,b}, N. Tosi^{a,b}, R. Travaglini^{a,b}

INFN Sezione di Catania ^a, Università di Catania ^b, CSFNSM ^c, Catania, Italy

S. Albergo^{a,b}, G. Cappello^a, M. Chiorboli^{a,b}, S. Costa^{a,b}, F. Giordano^{a,2}, R. Potenza^{a,b}, A. Tricomi^{a,b}, C. Tuve^{a,b}

INFN Sezione di Firenze ^a, Università di Firenze ^b, Firenze, Italy

G. Barbagli^a, V. Ciulli^{a,b}, C. Civinini^a, R. D'Alessandro^{a,b}, E. Focardi^{a,b}, E. Gallo^a, S. Gozzi^{a,b}, V. Gori^{a,b}, P. Lenzi^{a,b}, M. Meschini^a, S. Paoletti^a, G. Sguazzoni^a, A. Tropiano^{a,b}

INFN Laboratori Nazionali di Frascati, Frascati, Italy

L. Benussi, S. Bianco, F. Fabbri, D. Piccolo

INFN Sezione di Genova ^a, Università di Genova ^b, Genova, Italy

R. Ferretti^{a,b}, F. Ferro^a, M. Lo Vetere^{a,b}, E. Robutti^a, S. Tosi^{a,b}

INFN Sezione di Milano-Bicocca ^a, Università di Milano-Bicocca ^b, Milano, Italy

M.E. Dinardo^{a,b}, S. Fiorendi^{a,b}, S. Gennai^{a,2}, R. Gerosa^{a,b,2}, A. Ghezzi^{a,b}, P. Govoni^{a,b}, M.T. Lucchini^{a,b,2}, S. Malvezzi^a, R.A. Manzoni^{a,b}, A. Martelli^{a,b}, B. Marzocchi^{a,b,2}, D. Menasce^a, L. Moroni^a, M. Paganoni^{a,b}, D. Pedrini^a, S. Ragazzi^{a,b}, N. Redaelli^a, T. Tabarelli de Fatis^{a,b}

INFN Sezione di Napoli ^a, Università di Napoli 'Federico II' ^b, Napoli, Italy, Università della Basilicata ^c, Potenza, Italy, Università G. Marconi ^d, Roma, Italy

S. Buontempo^a, N. Cavallo^{a,c}, S. Di Guida^{a,d,2}, F. Fabozzi^{a,c}, A.O.M. Iorio^{a,b}, L. Lista^a, S. Meola^{a,d,2}, M. Merola^a, P. Paolucci^{a,2}

INFN Sezione di Padova ^a, Università di Padova ^b, Padova, Italy, Università di Trento ^c, Trento, Italy

P. Azzi^a, N. Bacchetta^a, D. Bisello^{a,b}, A. Branca^{a,b}, R. Carlin^{a,b}, P. Checchia^a, M. Dall'Osso^{a,b}, T. Dorigo^a, U. Dosselli^a, F. Gasparini^{a,b}, U. Gasparini^{a,b}, A. Gozzelino^a, K. Kanishchev^{a,c}, S. Lacaprara^a, M. Margoni^{a,b}, A.T. Meneguzzo^{a,b}, J. Pazzini^{a,b}, N. Pozzobon^{a,b}, P. Ronchese^{a,b}, F. Simonetto^{a,b}, E. Torassa^a, M. Tosi^{a,b}, P. Zotto^{a,b}, A. Zucchetta^{a,b}, G. Zumerle^{a,b}

INFN Sezione di Pavia ^a, Università di Pavia ^b, Pavia, Italy

M. Gabusi^{a,b}, S.P. Ratti^{a,b}, V. Re^a, C. Riccardi^{a,b}, P. Salvini^a, P. Vitulo^{a,b}

INFN Sezione di Perugia ^a, Università di Perugia ^b, Perugia, Italy

M. Biasini^{a,b}, G.M. Bilei^a, D. Ciangottini^{a,b,2}, L. Fanò^{a,b}, P. Lariccia^{a,b}, G. Mantovani^{a,b}, M. Menichelli^a, A. Saha^a, A. Santocchia^{a,b}, A. Spiezia^{a,b,2}

INFN Sezione di Pisa ^a, Università di Pisa ^b, Scuola Normale Superiore di Pisa ^c, Pisa, Italy

K. Androsov^{a,25}, P. Azzurri^a, G. Bagliesi^a, J. Bernardini^a, T. Boccali^a, G. Broccolo^{a,c}, R. Castaldi^a, M.A. Ciocci^{a,25}, R. Dell'Orso^a, S. Donato^{a,c,2}, G. Fedi, F. Fiori^{a,c}, L. Foà^{a,c}, A. Giassi^a, M.T. Grippo^{a,25}, F. Ligabue^{a,c}, T. Lomtadze^a, L. Martini^{a,b}, A. Messineo^{a,b}, C.S. Moon^{a,26}, F. Palla^{a,2}, A. Rizzi^{a,b}, A. Savoy-Navarro^{a,27}, A.T. Serban^a, P. Spagnolo^a, P. Squillacioti^{a,25}, R. Tenchini^a, G. Tonelli^{a,b}, A. Venturi^a, P.G. Verdini^a, C. Vernieri^{a,c}

INFN Sezione di Roma ^a, Università di Roma ^b, Roma, Italy

L. Barone^{a,b}, F. Cavallari^a, G. D'imperio^{a,b}, D. Del Re^{a,b}, M. Diemoz^a, C. Jorda^a, E. Longo^{a,b}, F. Margaroli^{a,b}, P. Meridiani^a, F. Micheli^{a,b,2}, G. Organtini^{a,b}, R. Paramatti^a, S. Rahatlou^{a,b}, C. Rovelli^a, F. Santanastasio^{a,b}, L. Soffi^{a,b}, P. Traczyk^{a,b,2}

INFN Sezione di Torino ^a, Università di Torino ^b, Torino, Italy, Università del Piemonte Orientale ^c, Novara, Italy

N. Amapane^{a,b}, R. Arcidiacono^{a,c}, S. Argiro^{a,b}, M. Arneodo^{a,c}, R. Bellan^{a,b}, C. Biino^a, N. Cartiglia^a, S. Casasso^{a,b,2}, M. Costa^{a,b}, R. Covarelli, A. Degano^{a,b}, N. Demaria^a, L. Finco^{a,b,2}, C. Mariotti^a, S. Maselli^a, E. Migliore^{a,b}, V. Monaco^{a,b}, M. Musich^a, M.M. Obertino^{a,c}, L. Pacher^{a,b}, N. Pastrone^a, M. Pelliccioni^a, G.L. Pinna Angioni^{a,b}, A. Potenza^{a,b}, A. Romero^{a,b}, M. Ruspa^{a,c}, R. Sacchi^{a,b}, A. Solano^{a,b}, A. Staiano^a, U. Tamponi^a

INFN Sezione di Trieste ^a, Università di Trieste ^b, Trieste, Italy

S. Belforte^a, V. Candelise^{a,b,2}, M. Casarsa^a, F. Cossutti^a, G. Della Ricca^{a,b}, B. Gobbo^a, C. La Licata^{a,b}, M. Marone^{a,b}, A. Schizzi^{a,b}, T. Umer^{a,b}, A. Zanetti^a

Kangwon National University, Chunchon, Korea

S. Chang, A. Kropivnitskaya, S.K. Nam

Kyungpook National University, Daegu, Korea

D.H. Kim, G.N. Kim, M.S. Kim, D.J. Kong, S. Lee, Y.D. Oh, H. Park, A. Sakharov, D.C. Son

Chonbuk National University, Jeonju, Korea

T.J. Kim, M.S. Ryu

Chonnam National University, Institute for Universe and Elementary Particles, Kwangju, Korea

J.Y. Kim, D.H. Moon, S. Song

Korea University, Seoul, Korea

S. Choi, D. Gyun, B. Hong, M. Jo, H. Kim, Y. Kim, B. Lee, K.S. Lee, S.K. Park, Y. Roh

Seoul National University, Seoul, Korea

H.D. Yoo

University of Seoul, Seoul, Korea

M. Choi, J.H. Kim, I.C. Park, G. Ryu

Sungkyunkwan University, Suwon, Korea

Y. Choi, Y.K. Choi, J. Goh, D. Kim, E. Kwon, J. Lee, I. Yu

Vilnius University, Vilnius, Lithuania

A. Juodagalvis

National Centre for Particle Physics, Universiti Malaya, Kuala Lumpur, Malaysia

J.R. Komaragiri, M.A.B. Md Ali, W.A.T. Wan Abdullah

Centro de Investigacion y de Estudios Avanzados del IPN, Mexico City, Mexico

E. Casimiro Linares, H. Castilla-Valdez, E. De La Cruz-Burelo, I. Heredia-de La Cruz, A. Hernandez-Almada, R. Lopez-Fernandez, A. Sanchez-Hernandez

Universidad Iberoamericana, Mexico City, Mexico

S. Carrillo Moreno, F. Vazquez Valencia

Benemerita Universidad Autonoma de Puebla, Puebla, Mexico

I. Pedraza, H.A. Salazar Ibarquen

Universidad Autónoma de San Luis Potosí, San Luis Potosí, Mexico

A. Morelos Pineda

University of Auckland, Auckland, New Zealand

D. Krofcheck

University of Canterbury, Christchurch, New Zealand

P.H. Butler, S. Reucroft

National Centre for Physics, Quaid-I-Azam University, Islamabad, Pakistan

A. Ahmad, M. Ahmad, Q. Hassan, H.R. Hoorani, W.A. Khan, T. Khurshid, M. Shoaib

National Centre for Nuclear Research, Swierk, Poland

H. Bialkowska, M. Bluj, B. Boimska, T. Frueboes, M. Górski, M. Kazana, K. Nawrocki, K. Romanowska-Rybinska, M. Szleper, P. Zalewski

Institute of Experimental Physics, Faculty of Physics, University of Warsaw, Warsaw, Poland

G. Brona, K. Bunkowski, M. Cwiok, W. Dominik, K. Doroba, A. Kalinowski, M. Konecki, J. Krolikowski, M. Misiura, M. Olszewski

Laboratório de Instrumentação e Física Experimental de Partículas, Lisboa, Portugal

P. Bargassa, C. Beirão Da Cruz E Silva, P. Faccioli, P.G. Ferreira Parracho, M. Gallinaro, L. Lloret Iglesias, F. Nguyen, J. Rodrigues Antunes, J. Seixas, J. Varela, P. Vischia

Joint Institute for Nuclear Research, Dubna, Russia

S. Afanasiev, P. Bunin, M. Gavrilenko, I. Golutvin, I. Gorbunov, A. Kamenev, V. Karjavin, V. Konoplyanikov, A. Lanev, A. Malakhov, V. Matveev²⁸, P. Moisezenz, V. Palichik, V. Perelygin, S. Shmatov, N. Skatchkov, V. Smirnov, A. Zarubin

Petersburg Nuclear Physics Institute, Gatchina (St. Petersburg), Russia

V. Golovtsov, Y. Ivanov, V. Kim²⁹, E. Kuznetsova, P. Levchenko, V. Murzin, V. Oreshkin, I. Smirnov, V. Sulimov, L. Uvarov, S. Vavilov, A. Vorobyev, An. Vorobyev

Institute for Nuclear Research, Moscow, Russia

Yu. Andreev, A. Dermenev, S. Gninenko, N. Golubev, M. Kirsanov, N. Krasnikov, A. Pashenkov, D. Tlisov, A. Toropin

Institute for Theoretical and Experimental Physics, Moscow, Russia

V. Epshteyn, V. Gavrilov, N. Lychkovskaya, V. Popov, I. Pozdnyakov, G. Safronov, S. Semenov, A. Spiridonov, V. Stolin, E. Vlasov, A. Zhokin

P.N. Lebedev Physical Institute, Moscow, Russia

V. Andreev, M. Azarkin³⁰, I. Dremin³⁰, M. Kirakosyan, A. Leonidov³⁰, G. Mesyats, S.V. Rusakov, A. Vinogradov

Skobeltsyn Institute of Nuclear Physics, Lomonosov Moscow State University, Moscow, Russia

A. Belyaev, E. Boos, M. Dubinin³¹, L. Dudko, A. Ershov, A. Gribushin, V. Klyukhin, O. Kodolova, I. Lokhtin, S. Obraztsov, S. Petrushanko, V. Savrin, A. Snigirev

State Research Center of Russian Federation, Institute for High Energy Physics, Protvino, Russia

I. Azhgirey, I. Bayshev, S. Bitioukov, V. Kachanov, A. Kalinin, D. Konstantinov, V. Krychkine, V. Petrov, R. Ryutin, A. Sobol, L. Tourtchanovitch, S. Troshin, N. Tyurin, A. Uzunian, A. Volkov

University of Belgrade, Faculty of Physics and Vinca Institute of Nuclear Sciences, Belgrade, Serbia

P. Adzic³², M. Ekmedzic, J. Milosevic, V. Rekovic

Centro de Investigaciones Energéticas Medioambientales y Tecnológicas (CIEMAT), Madrid, Spain

J. Alcaraz Maestre, C. Battilana, E. Calvo, M. Cerrada, M. Chamizo Llatas, N. Colino, B. De La Cruz, A. Delgado Peris, D. Domínguez Vázquez, A. Escalante Del Valle, C. Fernandez Bedoya, J.P. Fernández Ramos, J. Flix, M.C. Fouz, P. Garcia-Abia, O. Gonzalez Lopez, S. Goy Lopez, J.M. Hernandez, M.I. Josa, E. Navarro De Martino, A. Pérez-Calero Yzquierdo, J. Puerta Pelayo, A. Quintario Olmeda, I. Redondo, L. Romero, M.S. Soares

Universidad Autónoma de Madrid, Madrid, Spain

C. Albajar, J.F. de Trocóniz, M. Missiroli, D. Moran

Universidad de Oviedo, Oviedo, Spain

H. Brun, J. Cuevas, J. Fernandez Menendez, S. Folgueras, I. Gonzalez Caballero

Instituto de Física de Cantabria (IFCA), CSIC-Universidad de Cantabria, Santander, Spain

J.A. Brochero Cifuentes, I.J. Cabrillo, A. Calderon, J. Duarte Campderros, M. Fernandez, G. Gomez, A. Graziano, A. Lopez Virto, J. Marco, R. Marco, C. Martinez Rivero, F. Matorras, F.J. Munoz Sanchez, J. Piedra Gomez, T. Rodrigo, A.Y. Rodríguez-Marrero, A. Ruiz-Jimeno, L. Scodellaro, I. Vila, R. Vilar Cortabitarte

CERN, European Organization for Nuclear Research, Geneva, Switzerland

D. Abbaneo, E. Auffray, G. Auzinger, M. Bachtis, P. Baillon, A.H. Ball, D. Barney, A. Benaglia, J. Bendavid, L. Benhabib, J.F. Benitez, P. Bloch, A. Bocci, A. Bonato, O. Bondu, C. Botta, H. Breuker, T. Camporesi, G. Cerminara, S. Colafranceschi³³, M. D'Alfonso, D. d'Enterria, A. Dabrowski, A. David, F. De Guio, A. De Roeck, S. De Visscher, E. Di Marco, M. Dobson,

M. Dordevic, B. Dorney, N. Dupont-Sagorin, A. Elliott-Peisert, G. Franzoni, W. Funk, D. Gigi, K. Gill, D. Giordano, M. Girone, F. Glege, R. Guida, S. Gundacker, M. Guthoff, J. Hammer, M. Hansen, P. Harris, J. Hegeman, V. Innocente, P. Janot, K. Kousouris, K. Krajczar, P. Lecoq, C. Lourenço, N. Magini, L. Malgeri, M. Mannelli, J. Marrouche, L. Masetti, F. Meijers, S. Mersi, E. Meschi, F. Moortgat, S. Morovic, M. Mulders, L. Orsini, L. Pape, E. Perez, A. Petrilli, G. Petrucciani, A. Pfeiffer, M. Pimiä, D. Piparo, M. Plagge, A. Racz, G. Rolandi³⁴, M. Rovere, H. Sakulin, C. Schäfer, C. Schwick, A. Sharma, P. Siegrist, P. Silva, M. Simon, P. Sphicas³⁵, D. Spiga, J. Steggemann, B. Stieger, M. Stoye, Y. Takahashi, D. Treille, A. Tsirou, G.I. Veres¹⁷, N. Wardle, H.K. Wöhri, H. Wollny, W.D. Zeuner

Paul Scherrer Institut, Villigen, Switzerland

W. Bertl, K. Deiters, W. Erdmann, R. Horisberger, Q. Ingram, H.C. Kaestli, D. Kotlinski, U. Langenegger, D. Renker, T. Rohe

Institute for Particle Physics, ETH Zurich, Zurich, Switzerland

F. Bachmair, L. Bäni, L. Bianchini, M.A. Buchmann, B. Casal, N. Chanon, G. Dissertori, M. Dittmar, M. Donegà, M. Dünser, P. Eller, C. Grab, D. Hits, J. Hoss, W. Luster, M. Mangano, A.C. Marini, M. Marionneau, P. Martinez Ruiz del Arbol, M. Masciovecchio, D. Meister, N. Mohr, P. Musella, C. Nägeli³⁶, F. Nessi-Tedaldi, F. Pandolfi, F. Pauss, L. Perrozzi, M. Peruzzi, M. Quittnat, L. Rebane, M. Rossini, A. Starodumov³⁷, M. Takahashi, K. Theofilatos, R. Wallny, H.A. Weber

Universität Zürich, Zurich, Switzerland

C. AMSLER³⁸, M.F. Canelli, V. Chiochia, A. De Cosa, A. Hinzmann, T. Hreus, B. Kilminster, C. Lange, J. Ngadiuba, D. Pinna, P. Robmann, F.J. Ronga, S. Taroni, Y. Yang

National Central University, Chung-Li, Taiwan

M. Cardaci, K.H. Chen, C. Ferro, C.M. Kuo, W. Lin, Y.J. Lu, R. Volpe, S.S. Yu

National Taiwan University (NTU), Taipei, Taiwan

P. Chang, Y.H. Chang, Y. Chao, K.F. Chen, P.H. Chen, C. Dietz, U. Grundler, W.-S. Hou, Y.F. Liu, R.-S. Lu, M. Miñano Moya, E. Petrakou, Y.M. Tzeng, R. Wilken

Chulalongkorn University, Faculty of Science, Department of Physics, Bangkok, Thailand

B. Asavapibhop, G. Singh, N. Srimanobhas, N. Suwonjandee

Cukurova University, Adana, Turkey

A. Adiguzel, M.N. Bakirci³⁹, S. Cerci⁴⁰, C. Dozen, I. Dumanoglu, E. Eskut, S. Girgis, G. Gokbulut, Y. Guler, E. Gurpinar, I. Hos, E.E. Kangal⁴¹, A. Kayis Topaksu, G. Onengut⁴², K. Ozdemir⁴³, S. Ozturk³⁹, A. Polatoz, D. Sunar Cerci⁴⁰, B. Tali⁴⁰, H. Topakli³⁹, M. Vergili, C. Zorbilmez

Middle East Technical University, Physics Department, Ankara, Turkey

I.V. Akin, B. Bilin, S. Bilmis, H. Gamsizkan⁴⁴, B. Isildak⁴⁵, G. Karapinar⁴⁶, K. Ocalan⁴⁷, S. Sekmen, U.E. Surat, M. Yalvac, M. Zeyrek

Bogazici University, Istanbul, Turkey

E.A. Albayrak⁴⁸, E. Gülmez, M. Kaya⁴⁹, O. Kaya⁵⁰, T. Yetkin⁵¹

Istanbul Technical University, Istanbul, Turkey

K. Cankocak, F.I. Vardarli

National Scientific Center, Kharkov Institute of Physics and Technology, Kharkov, Ukraine

L. Levchuk, P. Sorokin

University of Bristol, Bristol, United Kingdom

J.J. Brooke, E. Clement, D. Cussans, H. Flacher, J. Goldstein, M. Grimes, G.P. Heath, H.F. Heath, J. Jacob, L. Kreczko, C. Lucas, Z. Meng, D.M. Newbold⁵², S. Paramesvaran, A. Poll, T. Sakuma, S. Seif El Nasr-storey, S. Senkin, V.J. Smith

Rutherford Appleton Laboratory, Didcot, United Kingdom

K.W. Bell, A. Belyaev⁵³, C. Brew, R.M. Brown, D.J.A. Cockerill, J.A. Coughlan, K. Harder, S. Harper, E. Olaiya, D. Petyt, C.H. Shepherd-Themistocleous, A. Thea, I.R. Tomalin, T. Williams, W.J. Womersley, S.D. Worm

Imperial College, London, United Kingdom

M. Baber, R. Bainbridge, O. Buchmuller, D. Burton, D. Colling, N. Cripps, P. Dauncey, G. Davies, M. Della Negra, P. Dunne, A. Elwood, W. Ferguson, J. Fulcher, D. Futyan, G. Hall, G. Iles, M. Jarvis, G. Karapostoli, M. Kenzie, R. Lane, R. Lucas⁵², L. Lyons, A.-M. Magnan, S. Malik, B. Mathias, J. Nash, A. Nikitenko³⁷, J. Pela, M. Pesaresi, K. Petridis, D.M. Raymond, S. Rogerson, A. Rose, C. Seez, P. Sharp[†], A. Tapper, M. Vazquez Acosta, T. Virdee, S.C. Zenz

Brunel University, Uxbridge, United Kingdom

J.E. Cole, P.R. Hobson, A. Khan, P. Kyberd, D. Leggat, D. Leslie, I.D. Reid, P. Symonds, L. Teodorescu, M. Turner

Baylor University, Waco, USA

J. Dittmann, K. Hatakeyama, A. Kasmi, H. Liu, N. Pastika, T. Scarborough, Z. Wu

The University of Alabama, Tuscaloosa, USA

O. Charaf, S.I. Cooper, C. Henderson, P. Rumerio

Boston University, Boston, USA

A. Avetisyan, T. Bose, C. Fantasia, P. Lawson, C. Richardson, J. Rohlf, J. St. John, L. Sulak

Brown University, Providence, USA

J. Alimena, E. Berry, S. Bhattacharya, G. Christopher, D. Cutts, Z. Demiragli, N. Dhingra, A. Ferapontov, A. Garabedian, U. Heintz, E. Laird, G. Landsberg, M. Narain, S. Sagir, T. Sinthuprasith, T. Speer, J. Swanson

University of California, Davis, Davis, USA

R. Breedon, G. Breto, M. Calderon De La Barca Sanchez, S. Chauhan, M. Chertok, J. Conway, R. Conway, P.T. Cox, R. Erbacher, M. Gardner, W. Ko, R. Lander, M. Mulhearn, D. Pellett, J. Pilot, F. Ricci-Tam, S. Shalhout, J. Smith, M. Squires, D. Stolp, M. Tripathi, S. Wilbur, R. Yohay

University of California, Los Angeles, USA

R. Cousins, P. Everaerts, C. Farrell, J. Hauser, M. Ignatenko, G. Rakness, E. Takasugi, V. Valuev, M. Weber

University of California, Riverside, Riverside, USA

K. Burt, R. Clare, J. Ellison, J.W. Gary, G. Hanson, J. Heilman, M. Ivova Rikova, P. Jandir, E. Kennedy, F. Lacroix, O.R. Long, A. Luthra, M. Malberti, M. Olmedo Negrete, A. Shrinivas, S. Sumowidagdo, S. Wimpenny

University of California, San Diego, La Jolla, USA

J.G. Branson, G.B. Cerati, S. Cittolin, R.T. D'Agnolo, A. Holzner, R. Kelley, D. Klein, J. Letts, I. Macneill, D. Olivito, S. Padhi, C. Palmer, M. Pieri, M. Sani, V. Sharma, S. Simon, M. Tadel, Y. Tu, A. Vartak, C. Welke, F. Würthwein, A. Yagil, G. Zevi Della Porta

University of California, Santa Barbara, Santa Barbara, USA

D. Barge, J. Bradmiller-Feld, C. Campagnari, T. Danielson, A. Dishaw, V. Dutta, K. Flowers, M. Franco Sevilla, P. Geffert, C. George, F. Golf, L. Gouskos, J. Incandela, C. Justus, N. Mccoll, S.D. Mullin, J. Richman, D. Stuart, W. To, C. West, J. Yoo

California Institute of Technology, Pasadena, USA

A. Apresyan, A. Bornheim, J. Bunn, Y. Chen, J. Duarte, A. Mott, H.B. Newman, C. Pena, M. Pierini, M. Spiropulu, J.R. Vlimant, R. Wilkinson, S. Xie, R.Y. Zhu

Carnegie Mellon University, Pittsburgh, USA

V. Azzolini, A. Calamba, B. Carlson, T. Ferguson, Y. Iiyama, M. Paulini, J. Russ, H. Vogel, I. Vorobiev

University of Colorado at Boulder, Boulder, USA

J.P. Cumalat, W.T. Ford, A. Gaz, M. Krohn, E. Luiggi Lopez, U. Nauenberg, J.G. Smith, K. Stenson, S.R. Wagner

Cornell University, Ithaca, USA

J. Alexander, A. Chatterjee, J. Chaves, J. Chu, S. Dittmer, N. Eggert, N. Mirman, G. Nicolas Kaufman, J.R. Patterson, A. Ryd, E. Salvati, L. Skinnari, W. Sun, W.D. Teo, J. Thom, J. Thompson, J. Tucker, Y. Weng, L. Winstrom, P. Wittich

Fairfield University, Fairfield, USA

D. Winn

Fermi National Accelerator Laboratory, Batavia, USA

S. Abdullin, M. Albrow, J. Anderson, G. Apollinari, L.A.T. Bauerdick, A. Beretvas, J. Berryhill, P.C. Bhat, G. Bolla, K. Burkett, J.N. Butler, H.W.K. Cheung, F. Chlebana, S. Cihangir, V.D. Elvira, I. Fisk, J. Freeman, E. Gottschalk, L. Gray, D. Green, S. Grünendahl, O. Gutsche, J. Hanlon, D. Hare, R.M. Harris, J. Hirschauer, B. Hooberman, S. Jindariani, M. Johnson, U. Joshi, B. Klima, B. Kreis, S. Kwan[†], J. Linacre, D. Lincoln, R. Lipton, T. Liu, R. Lopes De Sá, J. Lykken, K. Maeshima, J.M. Marraffino, V.I. Martinez Outschoorn, S. Maruyama, D. Mason, P. McBride, P. Merkel, K. Mishra, S. Mrenna, S. Nahn, C. Newman-Holmes, V. O'Dell, O. Prokofyev, E. Sexton-Kennedy, A. Soha, W.J. Spalding, L. Spiegel, L. Taylor, S. Tkaczyk, N.V. Tran, L. Uplegger, E.W. Vaandering, R. Vidal, A. Whitbeck, J. Whitmore, F. Yang

University of Florida, Gainesville, USA

D. Acosta, P. Avery, P. Bortignon, D. Bourilkov, M. Carver, D. Curry, S. Das, M. De Gruttola, G.P. Di Giovanni, R.D. Field, M. Fisher, I.K. Furic, J. Hugon, J. Konigsberg, A. Korytov, T. Kypreos, J.F. Low, K. Matchev, H. Mei, P. Milenovic⁵⁴, G. Mitselmakher, L. Muniz, A. Rinkevicius, L. Shchutska, M. Snowball, D. Sperka, J. Yelton, M. Zakaria

Florida International University, Miami, USA

S. Hewamanage, S. Linn, P. Markowitz, G. Martinez, J.L. Rodriguez

Florida State University, Tallahassee, USA

J.R. Adams, T. Adams, A. Askew, J. Bochenek, B. Diamond, J. Haas, S. Hagopian, V. Hagopian, K.F. Johnson, H. Prosper, V. Veeraraghavan, M. Weinberg

Florida Institute of Technology, Melbourne, USA

M.M. Baarmand, M. Hohmann, H. Kalakhety, F. Yumiceva

University of Illinois at Chicago (UIC), Chicago, USA

M.R. Adams, L. Apanasevich, D. Berry, R.R. Betts, I. Bucinskaite, R. Cavanaugh, O. Evdokimov,

L. Gauthier, C.E. Gerber, D.J. Hofman, P. Kurt, C. O'Brien, I.D. Sandoval Gonzalez, C. Silkworth, P. Turner, N. Varelas

The University of Iowa, Iowa City, USA

B. Bilki⁵⁵, W. Clarida, K. Dilsiz, M. Haytmyradov, J.-P. Merlo, H. Mermerkaya⁵⁶, A. Mestvirishvili, A. Moeller, J. Nachtman, H. Ogul, Y. Onel, F. Ozok⁴⁸, A. Penzo, R. Rahmat, S. Sen, P. Tan, E. Tiras, J. Wetzel, K. Yi

Johns Hopkins University, Baltimore, USA

I. Anderson, B.A. Barnett, B. Blumenfeld, S. Bolognesi, D. Fehling, A.V. Gritsan, P. Maksimovic, C. Martin, M. Swartz, M. Xiao

The University of Kansas, Lawrence, USA

P. Baringer, A. Bean, G. Benelli, C. Bruner, J. Gray, R.P. Kenny III, D. Majumder, M. Malek, M. Murray, D. Noonan, S. Sanders, J. Sekaric, R. Stringer, Q. Wang, J.S. Wood

Kansas State University, Manhattan, USA

I. Chakaberia, A. Ivanov, K. Kaadze, S. Khalil, M. Makouski, Y. Maravin, L.K. Saini, N. Skhirtladze, I. Svintradze

Lawrence Livermore National Laboratory, Livermore, USA

J. Gronberg, D. Lange, F. Rebassoo, D. Wright

University of Maryland, College Park, USA

A. Baden, A. Belloni, B. Calvert, S.C. Eno, J.A. Gomez, N.J. Hadley, S. Jabeen, R.G. Kellogg, T. Kolberg, Y. Lu, A.C. Mignerey, K. Pedro, A. Skuja, M.B. Tonjes, S.C. Tonwar

Massachusetts Institute of Technology, Cambridge, USA

A. Apyan, R. Barbieri, K. Bierwagen, W. Busza, I.A. Cali, L. Di Matteo, G. Gomez Ceballos, M. Goncharov, D. Gulhan, M. Klute, Y.S. Lai, Y.-J. Lee, A. Levin, P.D. Luckey, C. Paus, D. Ralph, C. Roland, G. Roland, G.S.F. Stephans, K. Sumorok, D. Velicanu, J. Veverka, B. Wyslouch, M. Yang, M. Zanetti, V. Zhukova

University of Minnesota, Minneapolis, USA

B. Dahmes, A. Gude, S.C. Kao, K. Klapoetke, Y. Kubota, J. Mans, S. Nourbakhsh, R. Rusack, A. Singovsky, N. Tambe, J. Turkewitz

University of Mississippi, Oxford, USA

J.G. Acosta, S. Oliveros

University of Nebraska-Lincoln, Lincoln, USA

E. Avdeeva, K. Bloom, S. Bose, D.R. Claes, A. Dominguez, R. Gonzalez Suarez, J. Keller, D. Knowlton, I. Kravchenko, J. Lazo-Flores, F. Meier, F. Ratnikov, G.R. Snow, M. Zvada

State University of New York at Buffalo, Buffalo, USA

J. Dolen, A. Godshalk, I. Iashvili, A. Kharchilava, A. Kumar, S. Rappoccio

Northeastern University, Boston, USA

G. Alverson, E. Barberis, D. Baumgartel, M. Chasco, A. Massironi, D.M. Morse, D. Nash, T. Orimoto, D. Trocino, R.-J. Wang, D. Wood, J. Zhang

Northwestern University, Evanston, USA

K.A. Hahn, A. Kubik, N. Mucia, N. Odell, B. Pollack, A. Pozdnyakov, M. Schmitt, S. Stoynev, K. Sung, M. Velasco, S. Won

University of Notre Dame, Notre Dame, USA

A. Brinkerhoff, K.M. Chan, A. Drozdetskiy, M. Hildreth, C. Jessop, D.J. Karmgard, N. Kellams, K. Lannon, S. Lynch, N. Marinelli, Y. Musienko²⁸, T. Pearson, M. Planer, R. Ruchti, G. Smith, N. Valls, M. Wayne, M. Wolf, A. Woodard

The Ohio State University, Columbus, USA

L. Antonelli, J. Brinson, B. Bylsma, L.S. Durkin, S. Flowers, A. Hart, C. Hill, R. Hughes, K. Kotov, T.Y. Ling, W. Luo, D. Puigh, M. Rodenburg, B.L. Winer, H. Wolfe, H.W. Wulsin

Princeton University, Princeton, USA

O. Driga, P. Elmer, J. Hardenbrook, P. Hebda, S.A. Koay, P. Lujan, D. Marlow, T. Medvedeva, M. Mooney, J. Olsen, P. Piroué, X. Quan, H. Saka, D. Stickland², C. Tully, J.S. Werner, A. Zuranski

University of Puerto Rico, Mayaguez, USA

E. Brownson, S. Malik, H. Mendez, J.E. Ramirez Vargas

Purdue University, West Lafayette, USA

V.E. Barnes, D. Benedetti, D. Bortoletto, M. De Mattia, L. Gutay, Z. Hu, M.K. Jha, M. Jones, K. Jung, M. Kress, N. Leonardo, D.H. Miller, N. Neumeister, F. Primavera, B.C. Radburn-Smith, X. Shi, I. Shipsey, D. Silvers, A. Svyatkovskiy, F. Wang, W. Xie, L. Xu, J. Zablocki

Purdue University Calumet, Hammond, USA

N. Parashar, J. Stupak

Rice University, Houston, USA

A. Adair, B. Akgun, K.M. Ecklund, F.J.M. Geurts, W. Li, B. Michlin, B.P. Padley, R. Redjimi, J. Roberts, J. Zabel

University of Rochester, Rochester, USA

B. Betchart, A. Bodek, P. de Barbaro, R. Demina, Y. Eshaq, T. Ferbel, M. Galanti, A. Garcia-Bellido, P. Goldenzweig, J. Han, A. Harel, O. Hindrichs, A. Khukhunaishvili, S. Korjenevski, G. Petrillo, M. Verzetti, D. Vishnevskiy

The Rockefeller University, New York, USA

R. Ciesielski, L. Demortier, K. Goulios, C. Mesropian

Rutgers, The State University of New Jersey, Piscataway, USA

S. Arora, A. Barker, J.P. Chou, C. Contreras-Campana, E. Contreras-Campana, D. Duggan, D. Ferencek, Y. Gershtein, R. Gray, E. Halkiadakis, D. Hidas, S. Kaplan, A. Lath, S. Panwalkar, M. Park, S. Salur, S. Schnetzer, D. Sheffield, S. Somalwar, R. Stone, S. Thomas, P. Thomassen, M. Walker

University of Tennessee, Knoxville, USA

K. Rose, S. Spanier, A. York

Texas A&M University, College Station, USA

O. Bouhali⁵⁷, A. Castaneda Hernandez, S. Dildick, R. Eusebi, W. Flanagan, J. Gilmore, T. Kamon⁵⁸, V. Khotilovich, V. Krutelyov, R. Montalvo, I. Osipenko, Y. Pakhotin, R. Patel, A. Perloff, J. Roe, A. Rose, A. Safonov, I. Suarez, A. Tatarinov, K.A. Ulmer

Texas Tech University, Lubbock, USA

N. Akchurin, C. Cowden, J. Damgov, C. Dragoiu, P.R. Duder, J. Faulkner, K. Kovitanggoon, S. Kunori, S.W. Lee, T. Libeiro, I. Volobouev

Vanderbilt University, Nashville, USA

E. Appelt, A.G. Delannoy, S. Greene, A. Gurrola, W. Johns, C. Maguire, Y. Mao, A. Melo, M. Sharma, P. Sheldon, B. Snook, S. Tuo, J. Velkovska

University of Virginia, Charlottesville, USA

M.W. Arenton, S. Boutle, B. Cox, B. Francis, J. Goodell, R. Hirosky, A. Ledovskoy, H. Li, C. Lin, C. Neu, E. Wolfe, J. Wood

Wayne State University, Detroit, USA

C. Clarke, R. Harr, P.E. Karchin, C. Kottachchi Kankanamge Don, P. Lamichhane, J. Sturdy

University of Wisconsin, Madison, USA

D.A. Belknap, D. Carlsmith, M. Cepeda, S. Dasu, L. Dodd, S. Duric, E. Friis, R. Hall-Wilton, M. Herndon, A. Hervé, P. Klabbers, A. Lanaro, C. Lazaridis, A. Levine, R. Loveless, A. Mohapatra, I. Ojalvo, T. Perry, G.A. Pierro, G. Polese, I. Ross, T. Sarangi, A. Savin, W.H. Smith, D. Taylor, C. Vuosalo, N. Woods

†: Deceased

1: Also at Vienna University of Technology, Vienna, Austria

2: Also at CERN, European Organization for Nuclear Research, Geneva, Switzerland

3: Also at Institut Pluridisciplinaire Hubert Curien, Université de Strasbourg, Université de Haute Alsace Mulhouse, CNRS/IN2P3, Strasbourg, France

4: Also at National Institute of Chemical Physics and Biophysics, Tallinn, Estonia

5: Also at Skobeltsyn Institute of Nuclear Physics, Lomonosov Moscow State University, Moscow, Russia

6: Also at Universidade Estadual de Campinas, Campinas, Brazil

7: Also at Laboratoire Leprince-Ringuet, Ecole Polytechnique, IN2P3-CNRS, Palaiseau, France

8: Also at Joint Institute for Nuclear Research, Dubna, Russia

9: Also at Suez University, Suez, Egypt

10: Also at Cairo University, Cairo, Egypt

11: Also at Fayoum University, El-Fayoum, Egypt

12: Also at British University in Egypt, Cairo, Egypt

13: Now at Ain Shams University, Cairo, Egypt

14: Also at Université de Haute Alsace, Mulhouse, France

15: Also at Brandenburg University of Technology, Cottbus, Germany

16: Also at Institute of Nuclear Research ATOMKI, Debrecen, Hungary

17: Also at Eötvös Loránd University, Budapest, Hungary

18: Also at University of Debrecen, Debrecen, Hungary

19: Also at University of Visva-Bharati, Santiniketan, India

20: Now at King Abdulaziz University, Jeddah, Saudi Arabia

21: Also at University of Ruhuna, Matara, Sri Lanka

22: Also at Isfahan University of Technology, Isfahan, Iran

23: Also at University of Tehran, Department of Engineering Science, Tehran, Iran

24: Also at Plasma Physics Research Center, Science and Research Branch, Islamic Azad University, Tehran, Iran

25: Also at Università degli Studi di Siena, Siena, Italy

26: Also at Centre National de la Recherche Scientifique (CNRS) - IN2P3, Paris, France

27: Also at Purdue University, West Lafayette, USA

28: Also at Institute for Nuclear Research, Moscow, Russia

29: Also at St. Petersburg State Polytechnical University, St. Petersburg, Russia

30: Also at National Research Nuclear University 'Moscow Engineering Physics

Institute' (MEPhI), Moscow, Russia

31: Also at California Institute of Technology, Pasadena, USA

32: Also at Faculty of Physics, University of Belgrade, Belgrade, Serbia

33: Also at Facoltà Ingegneria, Università di Roma, Roma, Italy

34: Also at Scuola Normale e Sezione dell'INFN, Pisa, Italy

35: Also at University of Athens, Athens, Greece

36: Also at Paul Scherrer Institut, Villigen, Switzerland

37: Also at Institute for Theoretical and Experimental Physics, Moscow, Russia

38: Also at Albert Einstein Center for Fundamental Physics, Bern, Switzerland

39: Also at Gaziosmanpasa University, Tokat, Turkey

40: Also at Adiyaman University, Adiyaman, Turkey

41: Also at Mersin University, Mersin, Turkey

42: Also at Cag University, Mersin, Turkey

43: Also at Piri Reis University, Istanbul, Turkey

44: Also at Anadolu University, Eskisehir, Turkey

45: Also at Ozyegin University, Istanbul, Turkey

46: Also at Izmir Institute of Technology, Izmir, Turkey

47: Also at Necmettin Erbakan University, Konya, Turkey

48: Also at Mimar Sinan University, Istanbul, Istanbul, Turkey

49: Also at Marmara University, Istanbul, Turkey

50: Also at Kafkas University, Kars, Turkey

51: Also at Yildiz Technical University, Istanbul, Turkey

52: Also at Rutherford Appleton Laboratory, Didcot, United Kingdom

53: Also at School of Physics and Astronomy, University of Southampton, Southampton, United Kingdom

54: Also at University of Belgrade, Faculty of Physics and Vinca Institute of Nuclear Sciences, Belgrade, Serbia

55: Also at Argonne National Laboratory, Argonne, USA

56: Also at Erzincan University, Erzincan, Turkey

57: Also at Texas A&M University at Qatar, Doha, Qatar

58: Also at Kyungpook National University, Daegu, Korea